High-rate multi-GNSS attitude determination: experiments, comparisons with inertial measurement units and applications of GNSS rotational seismology to the 2011 Tohoku Mw9.0 earthquake

OPEN ACCESS
IOP Publishing
Measurement Science and Technology
Meas. Sci. Technol. **30** (2019) 024003 (23pp)
https://doi.org/10.1088/1361-6501/aaf987

High-rate multi-GNSS attitude determination: experiments, comparisons with inertial measurement units and applications of GNSS rotational seismology to the 2011 Tohoku Mw9.0 earthquake

Peiliang Xu[1], Yuanming Shu[2], Xiaoji Niu[2], Jingnan Liu[2], Wanqiang Yao[3] and Qijin Chen[2]

[1] Disaster Prevention Research Institute, Kyoto University, Uji, Kyoto 611-0011, Japan
[2] GNSS Research Center, Wuhan University, Wuhan 430071, People's Republic of China
[3] School of Geomatics, Xi'an University of Science and Technology, Xi'an, People's Republic of China

E-mail: pxu@rcep.dpri.kyoto-u.ac.jp

Received 28 September 2018, revised 11 December 2018
Accepted for publication 18 December 2018
Published 17 January 2019

Abstract

High-rate GNSS positioning has been widely investigated and applied in science and engineering. We extend it to high-rate attitude determination under a multi-GNSS constellation. A series of experiments of high-rate GNSS attitude determination has been conducted on a platform with three 50 Hz geodetic receivers and two high-grade inertial measurement units (IMU). The high-rate attitude solutions are computed for each of the multi-GNSS systems and the combined constellation by either using short baselines with correct ambiguity resolution or precise point positioning (PPP) and compared with the IMU measurements. In the case of a single GNSS system, the experimental results have shown that GPS is of the best accuracy, followed by GLONASS. The results with Beidou are the noisiest. The combined multi-GNSS constellation can significantly improve the high-rate attitude solutions from any single GNSS system alone, which is, in particular, most suitable for applications to any platform in slow or quasi-static motion. However, the improvement rate could depend on proper weightings of measurements from different GNSS systems in the dynamical experiments. The accuracy of baseline-based high-rate GNSS attitude solutions remains stable over time, while that of PPP-based solutions substantially degrades with time, as theoretically expected. Within a short period of time, the PPP-based high-rate yaw solutions with the combined multi-GNSS constellation are comparable in accuracy with those computed from baselines with correct ambiguity resolution in the dynamical experiments. The attitude results from either static or dynamical experiments have shown that high-rate GNSS attitude determination is sufficiently precise to measure rotatory motions. GNSS rotational seismology is applied to the 2011 Tohoku Mw9.0 earthquake, illustrating the potential of multi-GNSS to precisely detect seismic rotatory motions.

Keywords: attitude determination, GNSS rotational seismology, high-rate GNSS, multi-GNSS constellations, precise point positioning, Tohoku Mw9.0 earthquake

1. Introduction

Attitude is required for navigation, guidance and control of objects in motion such as spacecraft, aircraft, vehicles, ships and unmanned vehicles. It can be determined either by using onboard attitude sensors such as accelerometers, magnetometers and gyros (Grewal *et al* 2001, Gebre-Egziabher *et al* 2004, Crassidis *et al* 2007) or satellite-based and star-tracking geometrical methods (Cohen 1992, Lu 1995, Seeber 2003) or combined solutions of onboard sensors with geometrical methods. Onboard sensors of attitude measurement can be advantageously made of small size and are very precise over a certain period of time but can erroneously drift away. As a result, precise determination of attitude often introduces uncertain bias parameters and gets involved with uncertain stochastic models to describe such parameters and uncertain kinematic models (Crassidis *et al* 2007).

Global navigation satellite systems (GNSS) are a precise and reliable 10-state instrument or sensor of positioning, velocity, timing and attitude, as have been repeatedly proved and demonstrated experimentally since the inception of the global positioning system (Cohen 1992, Hofmann-Wellenhof *et al* 1992, Parkinson and Spilker 1996, Seeber 2003). In principle, GNSS use precise geometrical carrier phase observables between GNSS satellites and the receivers fixed on a platform to determine the attitude of the platform (Ellis and Creswell 1979, Evans 1986, Van Graas and Braasch 1991, Cohen 1992, Cohen *et al* 1993, Lu *et al* 1994, Cannon and Sun 1996, Lachapelle *et al* 1996, Park *et al* 2000, Ardalan and Rezvani 2015), though code observables can be very useful at the stage of integer ambiguity resolution. Thus, unlike accelerometers, magnetometers and gyros, GNSS attitude determination is free of drift biases. Due to its geometrical nature, the accuracy of GNSS attitude estimation depends on three basic factors: noise level of carrier phases observables, residual errors of systematic types, correct ambiguity resolution for carrier phase observables and the geometrical size of a platform (Cohen 1992, Parkinson and Spilker 1996). GNSS attitude determination has been successfully applied to a variety of science and engineering problems, for example, in marine and photogrammetric applications, flying aircraft and automatic landing, aerospace applications (Cohen 1992, Lu 1995, Cannon and Sun 1996, Lachapelle *et al* 1996, Juang and Huang 1997, Leite and Walter 2007, Gross *et al* 2012).

High-rate GNSS precise positioning has attracted much attention for almost two decades and found wide applications in various areas of science and engineering. Most of engineering and sports' applications are based on GNSS precise relative positioning, often aided with sensors such as accelerometers, magnetometers and gyros. In civil engineering applications, high-rate GNSS precise positioning has been applied to monitor dynamic deformation of tall structures/buildings and bridges (Lovse *et al* 1995, Kijewski-Correa *et al* 2006, Meng *et al* 2007, Psimoulis *et al* 2008, Moschas and Stiros 2011, 2014, Moschas and Stiros 2015, Im *et al* 2013, Kaloop and Kim 2014, Roberts and Tang 2017). When aided with low cost micro-electro-mechanical system (MEMS), high-rate GNSS precise positioning can be used to provide precise positioning for aircrafts (Bischof and Schön 2017) and to continuously measure positions, velocities, and other movement information on athletes and pedestrians in sports-related applications (Waegli and Skaloud 2009, Morrison *et al* 2012). In geophysical applications, high-rate GNSS precise positioning has been successfully applied to measure waveforms of earthquakes (Kouba 2003, Larson *et al* 2003, Genrich and Bock 2006, Grapenthin and Freymueller 2011). In the case of large earthquakes, as in the case of 2011 Tohoku Mw9.0 earthquake in Japan, no reference station can be assumed to remain unmoved during the earthquake. In this case, one will have to use high-rate GNSS precise point positioning (PPP) to measure the dynamical displacements of stations. GNSS PPP has been shown, experimentally and theoretically, to reach the accuracy level of 2–4 mm in the horizontal components and sub-centimeters in the vertical component within a short period of time (Xu *et al* 2013, Shu *et al* 2017) and has been successfully used for structural deformation monitoring (Yigit 2016).

Although high-rate GNSS precise positioning has been widely applied in civil engineering and earth sciences, this is not the case with high-rate GNSS attitude. The major purpose of this research is to extend the work of Xu *et al* (2013) to GNSS attitude measurement over a short period of time for potential applications to GNSS rotational seismology and beyond. Bearing in mind the recent advance of multi-GNSS systems, this work will be further extended to the case of multi-GNSS systems. More specifically, we will focus on the three aspects in our study. The first purpose is to investigate the performance of high-rate multi-GNSS attitude determination. Since rotational seismology has been a hot topic recently, as the second purpose, we will apply high-rate GNSS attitude determination methods to the 2011 Tohoku Mw9.0 earthquake. On the other hand, when accelerometers and/or inertial measurement units (IMU) are used with GNSS to measure dynamical motion and deformation of man-made structures, they are either simply used to provide mutual confirmation of measurement results with enhanced reliability (Meng *et al* 2007, Moschas and Stiros 2011, 2015) or integrated with GNSS to produce the combined solutions of positions and velocities (Roberts *et al* 2004, Waegli and Skaloud 2009, Bock *et al* 2011, Morrison *et al* 2012). In this latter case, it is often assumed implicitly that GNSS, accelerometers and IMU would all have the same scaling. Experiments have shown that waveforms computed from these sensors can be slightly different in scaling and should be calibrated to properly integrate data from these different types of sensors (Xu *et al* 2013, Bischof and Schön 2017). In the case of attitude determination, attitude solutions from IMU can be biased and drift away in the long term from GNSS attitude solutions (Cohen *et al* 1993, Grewal *et al* 2001, Gebre-Egziabher *et al* 2004, Crassidis *et al* 2007, Ardalan and Rezvani 2015). Since the bias issue can be important, theoretically and practically, in integration of multi-sensors, the third purpose of this research

is to further compare high-rate GNSS attitudes with those measured with IMU over a short period of time.

2. Methods of multi-GNSS attitude determination

GNSS attitude determination is to solve for the attitude parameters of a moving or stationary platform by using GNSS carrier phase geometrical observables of three or more antennas installed on the platform (Cohen 1992, 1996, Lu 1995). A GNSS attitude determination system is said to be dedicated if all the antennas on the platform use the identical oscillator, otherwise, such an attitude system is said to be non-dedicated (Lu *et al* 1994, Lu 1995, Cannon and Sun 1996). Although attitude can be represented by using any three independent angular parameters such as Euler angles, quaternion parameters with one constraint or the attitude (direction cosine) matrix with six constraints on the elements (Cohen 1992, 1996, Lu 1995), the most often used parameters in the navigation literature are the three Euler angles of roll, pitch and yaw, which are defined in the body frame with respect to the local North (N), East (E) and Down (D) directions or the NED frame (Grewal *et al* 2001, Cohen 1992, 1996, Lu 1995).

GNSS attitude solutions can be obtained either by using the GNSS-derived baselines or directly from raw GNSS carrier phase observables (Cohen 1992, 1996, Lu 1995). These two methods are essentially equivalent after ambiguity resolution according to the equivalence theorem of parameters in a linear or linearized (real-valued) Gauss–Markov model (Baksalary 1984). In this latter case, one will also have to simultaneously resolve the integer ambiguity unknowns of carrier phase observables. The simultaneous least squares (LS) solution of attitude and integer ambiguity unknowns has been symbolically based on the following mixed integer linear observational model (Parkinson and Spilker 1996, Teunissen 2012a, Xu 2015):

$$\mathbf{y} = \mathbf{A}\boldsymbol{\beta} + \mathbf{B}\mathbf{z} + \boldsymbol{\epsilon}, \tag{1}$$

where $\mathbf{y}$ is an n-dimensional vector of observations, whose elements are often the double differences of carrier phase observables between two satellites and two receivers in the case of attitude determination, $\mathbf{A}$ and $\mathbf{B}$ are $(n \times t)$ and $(n \times m)$ real-valued matrices of full column rank, respectively, $\boldsymbol{\beta}$ is a t-dimensional real-valued non-stochastic vector, i.e. $\boldsymbol{\beta} \in \mathcal{R}^t$, and $\mathcal{R}^t$ is defined as the t-dimensional real-valued space. $\mathbf{z}$ is an m-dimensional unknown integer vector, i.e. $\mathbf{z} \in \mathbb{Z}^m$, $\mathbb{Z}^m$ is the m-dimensional integer space. $\boldsymbol{\epsilon}$ is the error vector of the observations $\mathbf{y}$, which is often assumed to be of zero mean and variance-covariance matrix $\mathbf{W}^{-1}\sigma^2$, with $\mathbf{W}$ being a positive definite weighting matrix and σ^2 an unknown positive scalar or the (unknown) variance of unit weight.

In attitude determination, $\boldsymbol{\beta}$ can either consist of all the position correction unknowns of the slave antennas relative to the master/main antenna or directly stand for the unknown attitude parameters (Cohen 1992, Lu 1995, Teunissen 2012b). Very often, $\boldsymbol{\beta}$ may also consist of other unknowns for the correction of systematic errors such as ionospheric errors, tropospheric errors, hardware delay and/or system biases. In principle, the observational equation (1) apply mathematically to both a single GNSS system and multi-GNSS systems. Nevertheless, in the case of multi-GNSS constellations, $\boldsymbol{\beta}$ can include some nuisance bias parameters among different GNSS systems such as intra-system biases and different time scales. Although GNSS attitude determination has often been formulated with double difference carrier phases, Teunissen (2012b) recently proposed the idea of array-aided precise point positioning (PPP) to precisely estimate the positions of the array receivers and the attitude (Henkel 2015).

In principle, the integer LS method can be directly applied to (1) to resolve the integer parameters $\mathbf{z}$, as first described for GNSS precise relative positioning in geodesy by Teunissen (1995) and further significantly improved by Chang *et al* (2005) and Xu *et al* (2012). For more mathematical reports on integer LS and reduction, the reader is referred to Lenstra *et al* (1982), Fincke and Pohst (1985), Schnorr and Euchner (1994) and Xu (2001, 2006, 2012, 2013). Nevertheless, since the multi-antenna configuration can be measured precisely *a priori*, a number of baseline-constrained ambiguity resolution methods have been developed under the framework of GNSS attitude determination (Lu 1995, Wang *et al* 2009, Teunissen 2012a). After the ambiguity resolution, one can then go ahead to solely determine the attitude of the platform.

If the baselines of a GNSS attitude system are first estimated from carrier phase observables by using precise relative positioning and/or PPP, then one can directly use them to determine the attitude of the platform. Mathematically speaking, given a number of unit vectors in both the local level NED and body frames, say $(\mathbf{u}_1, \mathbf{u}_2, ..., \mathbf{u}_m)$ in the NED frame and $(\mathbf{b}_1, \mathbf{b}_2, ..., \mathbf{b}_m)$ in the body frame, we will then solve for the unknown attitude matrix $\mathbf{R}$ by minimizing the following objective function:

$$\min : \quad \sum_{i=1}^{m} w_i \|\mathbf{u}_i - \mathbf{R}\mathbf{b}_i\|^2, \tag{2a}$$

subject to the orthonormality condition:

$$\mathbf{R}^T\mathbf{R} = \mathbf{R}\mathbf{R}^T = \mathbf{I}_3, \tag{2b}$$

$$\det\{\mathbf{R}\} = 1, \tag{2c}$$

(Lu 1995), where w_i is a positive weighting scalar, $\det\{\mathbf{R}\}$ stands for the determinant of $\mathbf{R}$ and $\mathbf{I}_3$ is a (3×3) identity matrix. If the rotation matrix is first properly parameterized with, for example, three Euler angles, the conditions (2*b*) and (2*c*) are automatically satisfied, and one can then simply solve the unconstrained minimization problem (2*a*) for the three Euler angles. Lu (1995) also extended the minimization model (2) to fully account for the variance–covariance matrices of both $\mathbf{u}_i$ and $\mathbf{b}_i$.

The optimization problem (2) was posed by Wahba (1965) under a more general condition without constraining $\mathbf{u}_i$ and $\mathbf{b}_i$ to unit vectors. If the condition (2*c*) of rotation is not

considered, namely, if **R** of (2) is only required to be orthogonal, the ordinary LS solution of **R** was actually solved analytically by Schönemann (1964) in his 1964 dissertation (see also Schönemann 1966), which is also known as the orthogonal procrustes problem. If the rotation matrix is desired, the orthonormal matrix of Schönemann (1966) will have to be adjusted to satisfy the condition of rotation.

Given a set of GNSS baseline solutions resolved with each of multi-GNSS constellations and the corresponding vectors in the body frame, there exist three major classes of methods to solve the weighted attitude problem (2): the R-method, the Y-method and the q-method. The R-method is to directly solve for the rotation matrix by using singular value decomposition (SVD) (Farrell and Stuelpnagel 1966), though the solution approach by Farrell and Stuelpnagel (1966) applies to problems of arbitrary dimension. In the case of 3D-rigid motion, the closed-form solution of the rotation matrix was also given by Arun *et al* (1987) and Horn *et al* (1988). If data are highly corrupted, Umeyama (1997) showed that the analytical solution with the R-method through SVD could fail and provided an improved solution. The Y-method was first proposed by Davenport (1968) and well documented in Keat (1977). The q-method, as its name stands, is to represent the rotation by using the quaternion parameters. It was first proposed by Davenport (see Keat 1977). Different variants of the q-method includes the TRIAD algorithm (Black 1964, Markley 2002), the QUEST algorithm (Shuster and Oh 1981) and the optimal and fast quaternion estimators (Markley and Mortari 2000). However, if the vectors $\mathbf{u}_i$ and $\mathbf{b}_i$ are not stochastically independent and/or if their elements are of different accuracy, one cannot obtain the closed-form solution of attitude but has to numerically solve for the attitude iteratively (Kanatani and Niitsuma 2012). Furthermore, if other data from IMU sensors are available, one can construct the optimal Kalman filtering of attitude (Shuster 1990, Gebre-Egziabher *et al* 2004, Crassidis *et al* 2007, Gross *et al* 2012).

Recently, Teunissen (2012b) proposed an array-aided PPP concept for simultaneous kinematic PPP positioning of an array and its attitude. The basic idea is to form a combined observational model, which consists of two sub-models: one with single difference (SD) observables of phases and codes between satellites for the array PPP and the other with double difference (DD) observables of phases and codes for the attitude determination of the array. The unknown parameters are treated separately but the correlations of the observables between the two sub-models are fully taken into account. Henkel (2015) followed the idea of Teunissen (2012b) to integrate SD observables of phases between satellites and an inertial sensor for PPP and attitude determination. Since the major purpose of Henkel (2015) was mainly for navigation applications, the tightly integrated system of PPP and attitude was required to be of low cost. As a result, only two low-cost single frequency GNSS receivers are used together with an IMU sensor to determine the attitude of the platform.

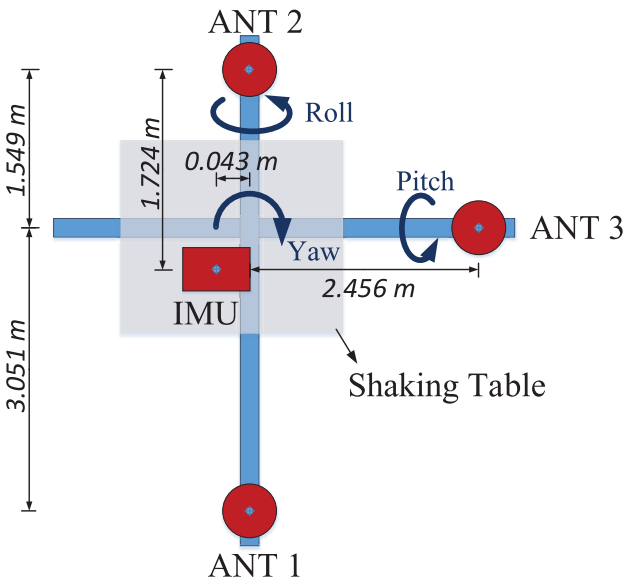

Figure 1. The schematic plot of the three Trimble Net R9 receivers/antennas and the IMU-FSAS inertial measurement unit in the experiments of high-rate GNSS attitude determination with multi-GNSS systems.

3. High-rate multi-GNSS experiments of attitude determination and comparison with IMU

High-rate GNSS experiments of attitude determination with multi-GNSS constellations were carried out twice on the roof of a 16-story building inside the information science campus of Wuhan University with three Trimble Net R9 receivers/antennas on March 22 and August 22, 2014, respectively. The schematic plot of three Trimble Net R9 receivers (Ant1, Ant2 and Ant3) for the experiments on March 22, 2014 is shown in figure 1. The three GNSS antennas are firmly fixed to the shake table (grey squares) constructed for the experiments of high-rate PPP with two almost orthogonal aluminium bars, each being of a length of about 4 m, rectangular size (8.44 cm × 4.90 cm) and thickness of about 0.18–0.20 cm, as shown in thick blue lines in figure 1. The three baselines between antennas are equal to 4.60 m (Ant1 and Ant2), 3.92 m (Ant1 and Ant3) and 2.90 m (Ant2 and Ant3), respectively, and the receivers are operational at the sampling rate of 50 Hz. For the comparative purpose, we have installed an IMU-FSAS inertial measurement unit on the shake table, which is also shown in figure 1 and supposed to measure roll, pitch and yaw at the accuracy of 29″, 29″ and 43″, respectively, as specified by its maker. The sampling rate of this IMU is 200 Hz. The experiments on August 22, 2014 basically followed the same setting as that on March 22, 2014, though the baselines between antennas are slightly different and the IMU has been replaced with one made by a different maker. The major configurations of GPS, Beidou, GLONASS and Galileo satellites during the experiments of March 22 and August 22 are plotted in figure 2.

In the experiments on August 22, we did not have any difficulty in tracking GNSS satellites. However, in the experiments

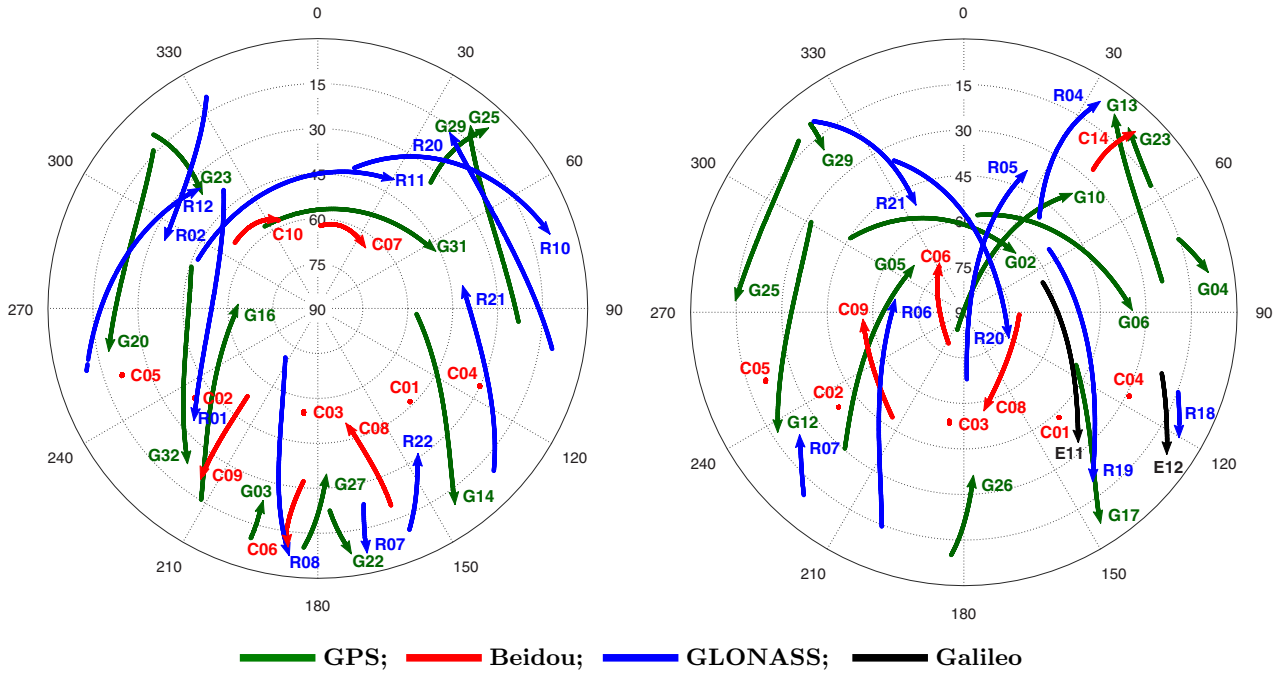

Figure 2. The sky plots of GNSS satellites for the experiments on March 22 (left plot) and August 22 (right plot), respectively. Note that since Galileo satellites was tracked only at Ant2 and of no use in the experiments of March 22, they are not shown on the left plot.

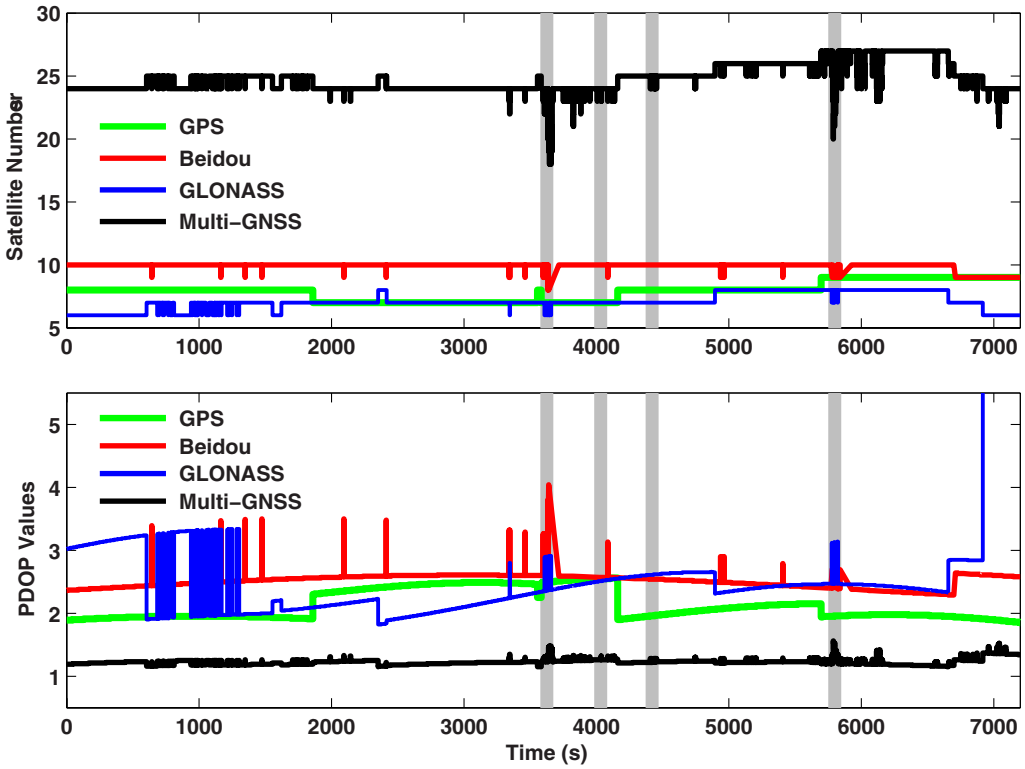

Figure 3. The satellite numbers and the PDOP values of GPS, Beidou, GLONASS and their combined multi-GNSS constellation at Ant1 during the experiments of high-rate attitude determination with multi-GNSS systems on March 22. The upper and lower panels show the numbers of satellites for each GNSS system and the corresponding PDOP values, respectively. The periods of the dynamical experiments are shown in grey bars.

of March 22, we did encounter some problems in locking on satellites, in particular, Beidou and Galileo satellites. More specifically, BeiDou C02 satellite could not be tracked by Ant3. A more serious problem is that after starting the first shaking experiment (at about 16:20:00, local time), Ant3 often failed to lock on and track BeiDou satellites C04, C05, C06 and C09. Although Ant2 successfully tracked two Galileo satellites, none of these two Galileo satellites were visible to

Ant1 and Ant3. As a result, Galileo satellites cannot be used and will not be reported in the following experiments on March 22. The satellite numbers and the PDOP values of each GNSS system and the combined multi-GNSS constellation at Ant1 are shown in figure 3, which are reasonably good during the experiments on March 22, with 7–9 satellites for GPS, 8–10 satellites for Beidou, and 6–8 satellites for GLONASS, respectively. The PDOP value of GPS is roughly slightly larger than 2.0 in most of the time, which is better than the other two systems Beidou and GLONASS. In the static experiments on August 22, the number of satellites for each of the multi-GNSS constellations is generally smaller than that on March 22. The number of satellites and the PDOP values will not be shown here. We should note, however, that during the dynamical experiments on March 22, Beidou system failed to determine dynamical attitudes by itself, due to the loss of tracking to five Beidou satellites at Ant3, as mentioned in the above.

Although the experiments on March 22 had more problems than those on August 22, the results showed some peculiar aspects when compared with those on August 22. More specifically, most Beidou satellites lose locking at Ant3 soon after starting the first dynamical experiment such that Beidou cannot afford to determine the attitude of the platform by itself. On the other hand, GLONASS performs reasonably well when compared with GPS. Thus, we choose to report mainly the results from these experiments in this paper. Nevertheless, we believe that the results from both experiments complement each other to help the reader better understand the advantages and potential problems of multi-GNSS attitude determination. We will also include the results of the experiments on August 22 for the purpose of comparison. In what follows, unless specified, the reported results are referred to the experiments on March 22. We should also note that the multi-GNSS attitude solution is derived by combining all the carrier phase measurements from different GNSS systems.

3.1. High-rate multi-GNSS baseline-based attitude determination: static experiments

To demonstrate the highest possible accuracy and potential problems of high-rate GNSS attitude determination, either with a single or multi-GNSS constellation, we have determined the high-rate attitudes of the platform with carrier phases in relative positioning mode by correctly resolving the integer ambiguities. More precisely, we have followed the two-step procedure to determine the attitudes of the platform by first correctly resolving the integer ambiguities of carrier phase observables, computing the baselines among the three antennas and then applying the formulation (2) to compute the rotation matrix $\mathbf{R}$ of attitude, with all the weightings w_i in (2) set to unity. Since static and kinematic GNSS solutions in precise (relative or absolute) positioning have been well known to be of different performances, we have designed the experiments to investigate both static and kinematic attitude solutions of the platform. In the case of kinematic attitude solutions, we will compare high-rate GNSS attitudes with those output from the installed IMU on the platform, since no true values of attitudes are available as a standard reference datum.

As the first part of the experiments on March 22, we have computed the high-rate GNSS attitudes of the static platform for each of the GNSS systems, namely, GPS, Beidou and GLONASS. However, the data are processed in kinematic mode by treating the motionless platform as if it were in motion. The major purpose of this static test is to demonstrate the accuracy of high-rate GNSS attitude determination with each of the multi-GNSS systems and to see how much improvement could be achieved by combining the multi-GNSS constellations. Shown in figure 4 are the high-rate GNSS attitudes determined with each of the multi-GNSS systems, namely, GPS (green lines), Beidou (red lines), GLONASS (blue lines) and their combined multi-GNSS solutions (black lines). To clearly visualize the high-rate attitude solutions with each of the GNSS systems and the combined solutions, we have added some constant shift values to the computed attitudes of yaw, pitch and roll in figure 4. As can be seen roughly from the widths and fluctuations of the lines in figure 4, the errors of GPS are the lowest, followed by GLONASS and then Beidou. We may qualitatively conclude that GPS has the best performance of high-rate attitude determination. Beidou looks like performing better than GLONASS in the component of yaw but clearly worse in the component of roll, as can be inferred from the levels of random errors and line fluctuations of figure 4. A quantitative analysis of the error statistics of these solutions from different GNSS constellations will be given later in this subsection.

The pattern of the best performances of GPS remains basically unchanged with the static results of the experiments on August 22, which are shown in figure 5. The best results of GPS from both experiments may be explained by the smallest errors of GPS measurements on one hand and likely a smaller PDOP value on the other hand. If we compare the respective results of Beidou (red lines) and GLONASS (blue lines) in figures 4 and 5, we may find that the widths of the Beidou (red) lines are consistently larger than those of the GLONASS (blue) lines but the GLONASS results show more wave-like motions, indicating that (i) the errors of Beidou are higher than GLONASS and (ii) the GLONASS attitude solutions contain some un-modelled or unknown wave-like errors in both experiments. In the case of the multi-GNSS constellation (GPS, Beidou, GLONASS and Galileo), the combined attitude solutions significantly outperform any of the attitude solutions from any single GNSS system in the experiments of March 22, as can also be seen from figure 4. However, they are only slightly better than the attitude solutions from GPS in the experiments on August 22 (compare figure 5). The static experimental attitude solutions on both March 22 and August 22 may imply that the combined multi-GNSS attitude solutions are not necessarily always much better than any single GNSS system. Instead, both experiments may actually suggest that potential improvement of a multi-GNSS constellation depend on the random errors of measurements of different GNSS systems or proper weightings of measurements from different GNSS systems, the number of satellites for each GNSS system and the corresponding PDOP values.

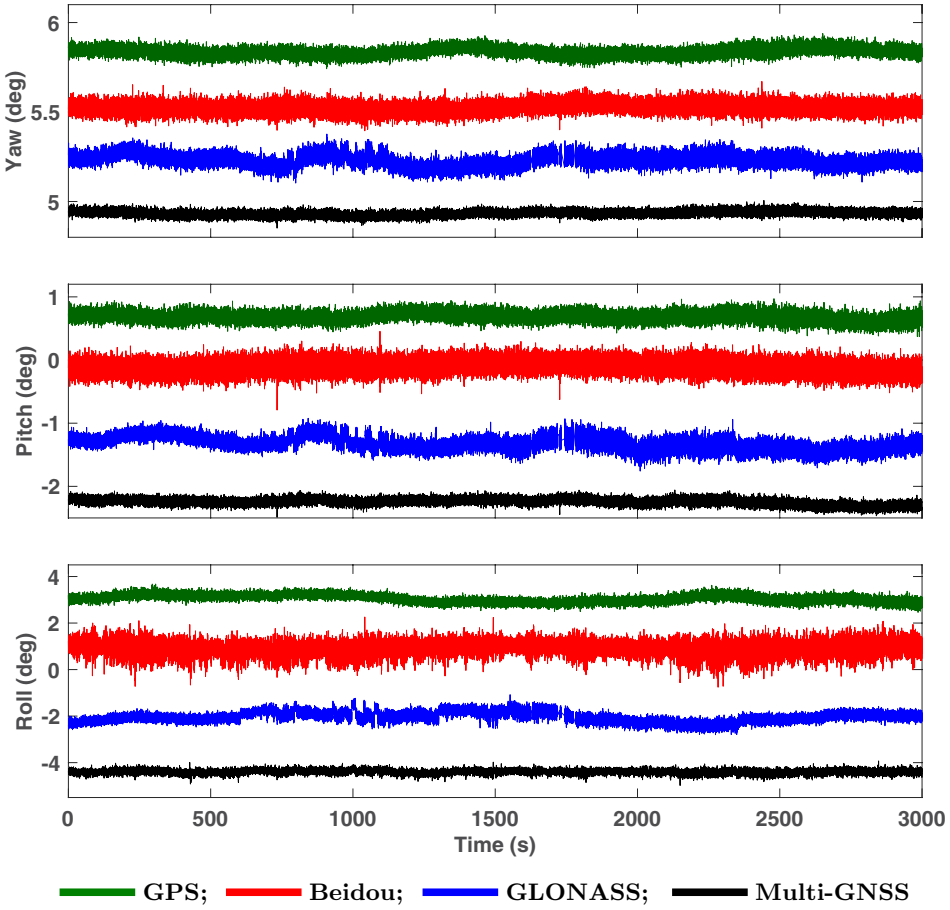

Figure 4. The high-rate, baseline-based GNSS static attitude solutions of March 22 determined with each of the multi-GNSS systems (GPS, Beidou, GLONASS) and their combined multi-constellation. To visualize clearly the attitude solutions with each of the GNSS systems and the combined solutions, we have added some constant shift values to the attitude solutions obtained.

To be quantitatively more precise, we have used the static high-rate GNSS attitude solutions from the experiments of March 22 and August 22 to compute the standard deviations of yaw, pitch and roll angles. To see and understand the short- and long-term accuracy behaviors of high-rate attitude solutions, we have also used the static attitude solutions to compute the standard deviations of attitudes with a different length of data ranging from 1 to 50 min from each of the multi-GNSS systems and the combined constellation, respectively, which are listed in tables 1 (March 22) and 2 (August 22), respectively. Error behaviors over a short period of time can be important in GNSS seismology, since no earthquakes rupture longer than 5 min up to the present. The results in these two tables have consistently shown that the accuracy of the high-rate attitude solutions computed with precise baselines remains almost unchanged with time, even though some larger standard deviations can sometimes be clearly observed (compare the accuracy from 20 to 50 min in the GPS baseline-based attitude solutions listed in table 2).

To correctly understand the error statistics of solutions from different GNSS systems, we limit ourselves to the static attitude results up to 5 min in tables 1 and 2. As can be seen, the GPS and Beidou solutions are of the lowest and highest levels of errors, respectively, with those of GLONASS in between, which has confirmed our qualitative analysis in the above from a quick look at and simple comparison of the widths of the corresponding lines in figures 4 and 5. More precisely, the GPS attitude solutions remain the best in all the three components of yaw, pitch and roll with all the lengths of data. If we limit ourselves to the first 5 min data, GPS is, on average, better than Beidou by a factor of about 42 percent in yaw, 48 percent in pitch and 120 percent in roll for the experiments on March 22, respectively. GPS is about 32 percent better than GLONASS in yaw but roughly the same as GLONASS in both pitch and roll. In the experiments on August 22, the average improvement rates of GPS over Beidou over the first 5 min become 130 percent in yaw, 71 percent in pitch and 129 percent in roll, respectively. GLONASS performs better than Beidou by an average of 44 percent in yaw, 64 percent in pitch and 46 percent in roll, respectively.

With the increasing length of data, the static experiments of August 22 have revealed some mixed features, as can be seen from table 2. Beidou seems to perform slightly better sometimes than GPS and GLONASS in some of the components. This phenomenon of accuracy between Beidou and GLONASS may likely be due to some unknown error sources in the GLONASS measurements that cause the wave-like motions in the GLONASS attitude solutions, as analyzed qualitatively in the above and seen from figures 4 and 5. On the other hand, table 2 has shown that the standard deviations

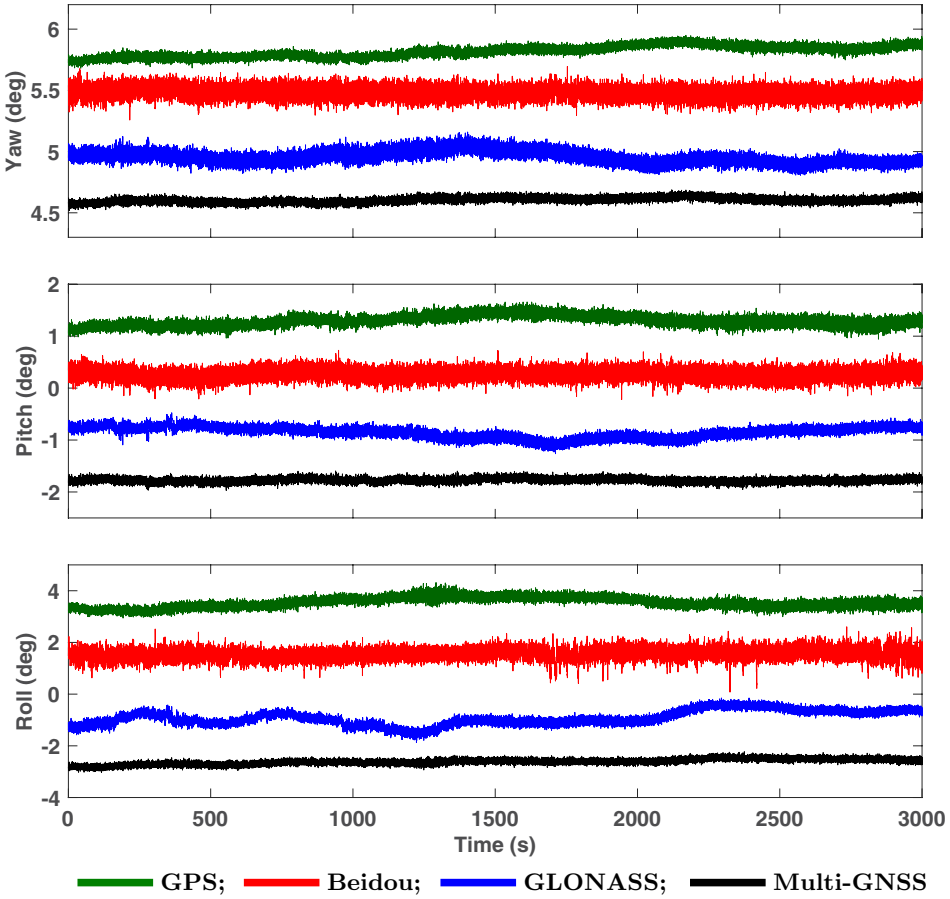

Figure 5. The high-rate, baseline-based GNSS static attitude solutions of August 22 determined with each of the multi-GNSS systems (GPS, Beidou, GLONASS) and their combined multi-constellation. The two Galileo satellites have been incorporated into the multi-GNSS solutions.

Table 1. The standard deviations (deg) of the attitude solutions with the multi-GNSS systems during the static period of the experiments on March 22 by using either precise relative positioning or precise point positioning. The column 'multi-GNSS' refers to the combined attitude solution with the multi-GNSS constellation.

Systems	GPS			Beidou			GLONASS			Multi-GNSS		
Attitudes	Yaw	Pitch	Roll	Yaw	Pitch	Roll	Yaw	Pitch	Roll	Yaw	Pitch	Roll
Precise relative positioning												
1 min	0.017	0.058	0.091	0.023	0.086	0.197	0.021	0.049	0.090	0.012	0.037	0.074
3 min	0.017	0.059	0.103	0.025	0.087	0.238	0.023	0.054	0.105	0.012	0.038	0.081
5 min	0.018	0.061	0.128	0.026	0.090	0.274	0.025	0.068	0.127	0.013	0.038	0.084
10 min	0.021	0.062	0.117	0.026	0.090	0.283	0.026	0.072	0.116	0.015	0.039	0.088
20 min	0.021	0.063	0.114	0.027	0.094	0.272	0.032	0.092	0.182	0.015	0.040	0.089
30 min	0.022	0.063	0.165	0.027	0.096	0.264	0.036	0.096	0.191	0.015	0.040	0.088
40 min	0.022	0.063	0.162	0.027	0.095	0.267	0.034	0.102	0.226	0.015	0.041	0.088
50 min	0.023	0.069	0.159	0.027	0.097	0.269	0.033	0.107	0.211	0.015	0.049	0.089
Precise point positioning												
1 min	0.030	0.113	0.196	0.066	0.213	0.398	0.088	0.236	0.469	0.031	0.103	0.125
3 min	0.033	0.155	0.337	0.078	0.197	0.646	0.101	0.228	0.482	0.030	0.093	0.301
5 min	0.034	0.148	0.467	0.077	0.191	0.602	0.103	0.224	0.465	0.032	0.110	0.266
10 min	0.053	0.297	0.382	0.079	0.191	0.605	0.131	0.291	0.525	0.037	0.158	0.245
20 min	0.047	0.293	0.392	0.094	0.218	0.610	0.173	0.423	0.587	0.044	0.143	0.280
30 min	0.048	0.262	0.402	0.080	0.234	0.564	0.206	0.578	1.570	0.049	0.177	0.300
40 min	0.053	0.277	0.361	0.074	0.261	0.586	0.315	1.072	1.501	0.049	0.239	0.321
50 min	0.067	0.259	0.373	0.078	0.291	0.795	0.292	0.979	1.403	0.051	0.229	0.331

Table 2. The standard deviations (deg) of the attitude solutions with the multi-GNSS systems during the static period of the experiments on August 22 by using either precise relative positioning or precise point positioning. The column 'multi-GNSS' refers to the combined attitude solution with the multi-GNSS constellation, with two Galileo satellites included in the multi-constellation.

Systems	GPS			Beidou			GLONASS			Multi-GNSS		
Attitudes	Yaw	Pitch	Roll	Yaw	Pitch	Roll	Yaw	Pitch	Roll	Yaw	Pitch	Roll
Precise relative positioning												
1 min	0.016	0.049	0.077	0.045	0.089	0.190	0.029	0.050	0.094	0.015	0.038	0.056
3 min	0.020	0.052	0.085	0.042	0.086	0.192	0.029	0.053	0.128	0.017	0.038	0.057
5 min	0.021	0.055	0.087	0.042	0.091	0.187	0.032	0.060	0.220	0.018	0.040	0.068
10 min	0.020	0.055	0.107	0.042	0.093	0.181	0.036	0.060	0.187	0.017	0.040	0.070
20 min	0.021	0.077	0.189	0.041	0.093	0.168	0.038	0.066	0.212	0.017	0.041	0.084
30 min	0.033	0.112	0.227	0.041	0.090	0.182	0.045	0.117	0.208	0.021	0.042	0.091
40 min	0.047	0.104	0.209	0.041	0.090	0.187	0.048	0.113	0.260	0.023	0.042	0.101
50 min	0.046	0.100	0.199	0.041	0.091	0.194	0.050	0.109	0.282	0.022	0.041	0.108
Precise point positioning												
1 min	0.033	0.080	0.164	0.083	0.120	0.180	0.074	0.193	0.410	0.033	0.079	0.155
3 min	0.031	0.075	0.171	0.083	0.164	0.201	0.084	0.165	0.492	0.032	0.079	0.208
5 min	0.031	0.101	0.188	0.090	0.203	0.195	0.088	0.181	0.417	0.033	0.088	0.193
10 min	0.035	0.210	0.191	0.083	0.325	0.211	0.086	0.182	0.501	0.035	0.192	0.199
20 min	0.044	0.177	0.259	0.131	0.396	0.227	0.281	0.299	0.832	0.062	0.191	0.197
30 min	0.060	0.189	0.591	0.153	0.354	0.265	0.319	0.358	0.831	0.060	0.238	0.209
40 min	0.068	0.184	0.634	0.157	0.356	0.353	0.328	0.345	0.952	0.064	0.245	0.260
50 min	0.070	0.252	0.592	0.196	0.472	0.383	0.332	0.360	1.251	0.064	0.235	0.252

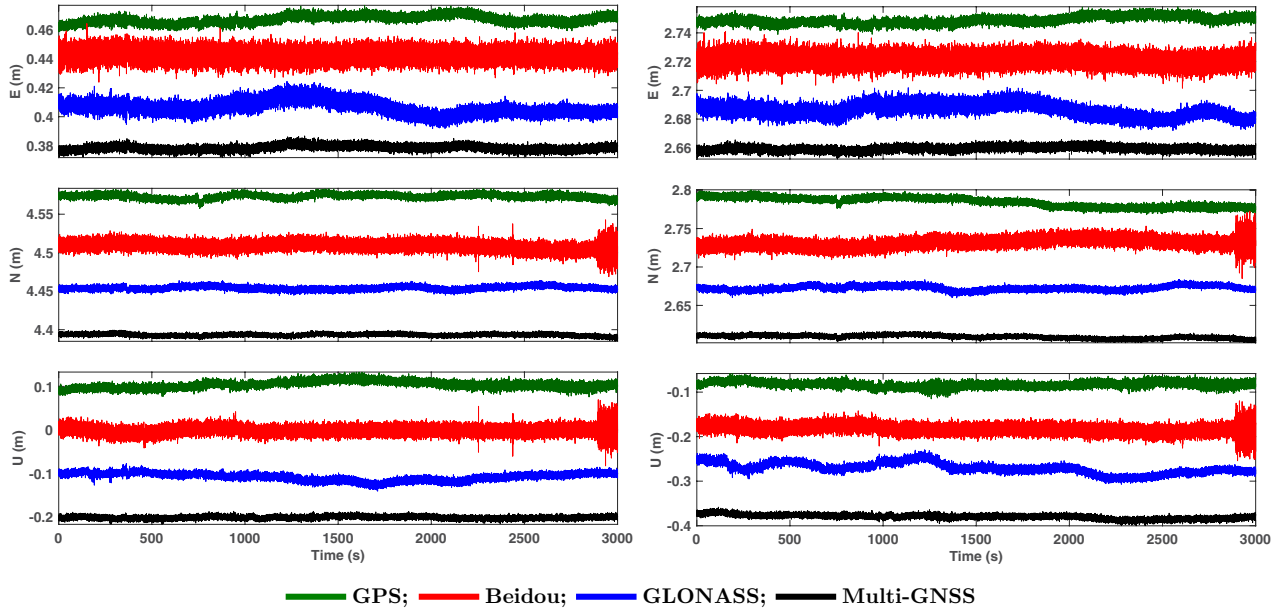

Figure 6. The baseline solutions after the integer ambiguity resolution with each of the multi-GNSS systems on August 22: left plot—baseline between Ant1 and Ant2; right plot—baseline between Ant 1 and Ant 3.

of GPS attitude solutions are larger than those of Beidou, when the length of data is more than 30 min. These larger standard deviations may not really imply an accuracy degradation in GPS baseline-based attitude solutions. Actually, after a careful look at figure 5, we can see a clear trend in both the yaw and pitch directions of GPS baseline-based attitude solutions, which also appears in the GPS baseline solutions of August 22, as shown in figure 6. The same trend can also be observed in the multi-GNSS solutions of attitudes and baselines in figures 5 and 6 but can hardly be identified in the Beidou and GLONASS solutions, because these latter solutions are too noisy to reveal such a small trend. The observed trend of GPS attitude solutions may more probably imply that the platform is subject to some small drift over time. Although the motion of the platform is very small, it may have been clearly observed in the baseline solutions in figure 6.

In addition to the error analysis, we have also computed the mean values of yaw, pitch and roll for each of the GNSS systems and the multi-GNSS constellation with the static experimental results on March 22 and August 22, which are listed in table 3. The mean values of pitch and roll with Beidou are significantly different from those with other GNSS systems on March 22. The reason remains unclear after carefully checking the computing software, the phase and code observables.

Noticing the fact that five Beidou GEO satellites are roughly distributed symmetrically around the long bar (Ant1–Ant2) of the experiment platform, we did some extra test computations with and without Beidou GEO satellites, indicating that the Beidou GEO satellites can significantly affect the mean attitudes of pitch and roll. More precisely, the mean attitudes of pitch and roll from Beidou without the five GEO satellites change to 0.910 and 2.509 degrees on March 22, and to 1.153 and 3.540 degrees on August 22, respectively. On the other hand, the mean values of pitch and roll with GLONASS are significantly different from those with other GNSS systems on August 22. The reason may be attributed to the wave-like fluctuations of baseline-based attitude solutions of the day, as explained in the above, whose maximum amplitude is much larger than the corresponding noise levels, in particular, in the roll component.

3.2. High-rate multi-GNSS baseline-based attitude determination: dynamical experiments and comparison with IMU

As the second part of the experiments, we would like to investigate the performances of high-rate GNSS attitude determinations for a platform in motion with each of the multi-GNSS systems and the combined constellation. More precisely, we have carried out four dynamical attitude experiments by pushing, pulling and/or shaking the platform. The first three dynamical experiments are controlled on purpose by mainly manipulating the platform to be subject to motion in a particular attitude direction, namely, with the order of yaw, pitch and roll, respectively. The fourth experiment is to set the platform to move freely in any of the three attitude directions. Since the true attitude values of the platform at any time epoch are unknown in dynamical experiments, we have installed a high grade IMU on the platform for the purpose of comparison. As in the case of high-rate PPP experiments reported in Xu *et al* (2013), there exist the problems of scaling and timing misalignment between GNSS and IMU, which have been computed after the procedure described in Xu *et al* (2013). The timing misalignments between GNSS and IMU have been found to be equal to 0.01 s for the two IMUs used on March 22 and August 22. However, the scaling factors between GNSS and these two IMUs are different and equal to 1.0940 for the IMU used on March 22 and 1.0266 for the other IMU on August 22, respectively. The scaling factors and timing misalignment between GNSS and IMU have been respectively applied to correct all the IMU-measured attitude data in the experiments on March 22 and August 22. We should note that due to likely flexure of the aluminium bars, the scaling factors of IMU relative to GNSS are determined by using only the measurements with the strongest signals from GNSS and IMU.

In what follows, we will report the results of baseline-based high-rate attitude determination on March 22 and August 22. We should note that due to the failure of locking to five Beidou satellites at Ant3 after starting the dynamical experiments on March 22, the number of Beidou satellites was not sufficient to determine the attitudes of the platform alone. As a result, no dynamical attitude results of Beidou alone were available on March 22.

Table 3. The mean values (deg) of the attitude solutions with the multi-GNSS systems during the static periods of the experiments on March 22 and August 22 by using precise relative positioning. 'Multi-GNSS' also includes two Galileo satellites on August 22.

GNSS systems	March 22 experiments			August 22 experiments		
	Yaw	Pitch	Roll	Yaw	Pitch	Roll
GPS	5.837	0.687	3.051	5.817	1.297	3.541
Beidou	5.825	0.894	3.389	5.882	1.268	3.558
GLONASS	5.830	0.681	2.956	5.755	1.147	3.079
Multi-GNSS	5.834	0.757	3.102	5.804	1.226	3.386

To evaluate the dynamical performances of the high-rate multi-GNSS attitude determination, we have computed the differences between the high-rate baseline-based GNSS attitude solutions and the IMU measurements during the four dynamical experiments and used them to directly compute the roots of mean squared errors for each of the multi-GNSS systems and the combined constellation. The results of error statistics for the dynamical experiments on March 22 are summarized and listed in table 4. Although the four dynamical experiments are conducted at different times, it is clear from table 4 that: (i) the accuracy of GPS, GLONASS and the multi-GNSS baseline-based attitude solutions is basically independent of time, though there are some small variations among the four dynamical experiments. This pattern is consistent with that of the static experiments and should be theoretically expected; (ii) since the accuracy of baseline-based static and dynamical solutions roughly remains unchanged with time on March 22, we compute the average accuracy of static solutions for all the three components of each GNSS system with the accuracy data in table 1 and the average accuracy of the four dynamical solutions with the accuracy data in table 4. The average accuracy of the static solutions is about 2.01, 1.26 and 0.74 times better than that of the dynamical ones in yaw, pitch and roll in the case of the GPS dynamical experiments, and 0.96, 0.75 and 0.85 times better in the case of the GLONASS dynamical experiments, respectively. On the other hand, although the GPS baseline-based static results are consistently better than those of GLONASS, GLONASS performs slightly better than GPS, basically in the yaw and pitch directions in the case of dynamical experiments, with a maximum improvement of 20.97 percent in the yaw of the fourth dynamical experiment on March 22; and (iii) the yaw solutions are best determined for each of the multi-GNSS systems. The average accuracy of yaw among the four dynamical experiments is about 1.32 and 2.73 times better than that of pitch and roll attitude solutions in the case of GPS, and about 1.57 and 4.14 times better in the case of GLONASS, respectively. The worst roll solutions may again be attributed to the short span of antennas along the roll direction, the poor accuracy of positioning in the vertical component and the flexure of the aluminium bars.

The accuracy of the combined multi-GNSS attitude solutions is listed in column 'multi-GNSS' of table 4, which includes GPS, GLONASS and Beidou. The combined attitude

Table 4. The standard deviations (deg) of the attitude differences between GNSS and IMU during the dynamic experiments on March 22 by using either precise relative positioning or precise point positioning. The column 'multi-GNSS' refers to the combined attitude solution with GPS, GLONASS and Beidou. The column 'GPS+GLONASS' refers to the combined attitude solution with only GPS and GLONASS. DynEx1, DynEx2, DynEx3 and DynEx4 refer to the four dynamical experiments, respectively.

Systems	GPS			GLONASS			Multi-GNSS			GPS+GLONASS		
Attitudes	Yaw	Pitch	Roll	Yaw	Pitch	Roll	Yaw	Pitch	Roll	Yaw	Pitch	Roll
Precise relative positioning												
DynEx1	0.057	0.147	0.208	0.070	0.134	0.358	0.052	0.095	0.225	0.049	0.088	0.211
DynEx2	0.063	0.157	0.261	0.050	0.177	0.292	0.052	0.185	0.262	0.052	0.153	0.246
DynEx3	0.060	0.105	0.214	0.056	0.102	0.269	0.054	0.088	0.210	0.055	0.087	0.204
DynEx4	0.062	0.153	0.222	0.049	0.148	0.235	0.049	0.139	0.209	0.050	0.133	0.190
Precise point positioning												
DynEx1	0.066	0.159	0.240	0.110	0.359	0.772	0.067	0.185	0.304	0.057	0.174	0.324
DynEx2	0.056	0.186	0.278	0.133	0.344	0.545	0.072	0.213	0.354	0.081	0.224	0.335
DynEx3	0.059	0.146	0.326	0.099	0.256	0.558	0.062	0.124	0.343	0.071	0.144	0.359
DynEx4	0.071	0.156	0.302	0.094	0.581	0.563	0.073	0.286	0.394	0.069	0.194	0.328

Table 5. The standard deviations (deg) of the attitude differences between GNSS and IMU during the dynamic experiments on August 22 by using either precise relative positioning or precise point positioning. The column 'multi-GNSS' refers to the combined attitude solutions with GPS, Beidou and GLONASS, together with two Galileo satellites. DynEx1, DynEx2, DynEx3 and DynEx4 refer to the four dynamical experiments, respectively.

Systems	GPS			Beidou			GLONASS			Multi-GNSS		
Attitudes	Yaw	Pitch	Roll	Yaw	Pitch	Roll	Yaw	Pitch	Roll	Yaw	Pitch	Roll
Precise relative positioning												
DynEx1	0.079	0.106	0.190	0.110	0.127	0.391	0.089	0.089	0.192	0.077	0.072	0.137
DynEx2	0.050	0.138	0.186	0.064	0.193	0.330	0.064	0.132	0.188	0.041	0.107	0.136
DynEx3	0.044	0.084	0.292	0.052	0.133	0.532	0.050	0.081	0.321	0.036	0.067	0.289
DynEx4	0.088	0.164	0.271	0.120	0.292	0.582	0.089	0.169	0.316	0.079	0.129	0.221
Precise point positioning												
DynEx1	0.127	0.191	0.385	0.172	0.629	1.177	0.202	0.201	0.683	0.126	0.147	0.330
DynEx2	0.101	0.236	0.359	0.135	0.618	1.233	0.101	0.226	0.420	0.066	0.184	0.302
DynEx3	0.087	0.124	0.494	0.143	0.243	3.859	0.146	0.198	0.573	0.070	0.144	0.439
DynEx4	0.127	0.236	0.559	0.225	0.862	2.043	0.349	0.816	1.334	0.111	0.289	0.519

solutions are generally better than those from any single GNSS system. Since locking was lost on several Beidou satellites in the dynamical experiments on March 22 and since the static results from Beidou have been found to be the noisiest, we have also computed the baseline-based attitudes for the dynamical experiments with only GPS and GLONASS by leaving Beidou out, whose accuracy is listed in column 'GPS+GLONASS' in table 4. The results without Beidou obviously are slightly better than those with Beidou. On average, the multi-GNSS attitude solutions without Beidou are more accurate than those with Beidou by 0.58, 8.63 and 6.52 percent in yaw, pitch and roll, respectively. The combined solutions with only GPS and GLONASS improve those of GPS-only solutions in accuracy by 17.64, 26.35 and 6.61 percent in yaw, pitch and roll, and those of GLONASS-only solutions by 9.71, 24.12 and 35.98 percent, respectively. However, one may see that sometimes, a negligible degradation can be found in the roll component of the first dynamical experiment, which may imply that equal weights for all the phase measurements from different GNSS systems may not be appropriate and variance component estimation should probably be incorporated in the future.

In the dynamical experiments on August 22, we have listed the accuracy of the four dynamical baseline-based attitude solutions in table 5. The error patterns observed from the dynamical multi-GNSS data of March 22 basically still remain valid, though the accuracy of solutions changes somehow. More precisely, on average, the combined multi-GNSS baseline-based attitude solutions are now better than those with GPS by 14.54, 32.17 and 24.78 percent in yaw, pitch and roll, with Beidou by 48.82, 95.41 and 143.87 percent, and with GLONASS by 30.81, 24.72 and 33.11 percent, respectively. To compare the performances of different GNSS systems, both GPS and GLONASS perform consistently much better than Beidou with the four dynamical experiments in all the attitude directions, with an average improvement of 30.45, 49.01 and 95.04 percent in yaw, pitch and roll for GPS, and 15.61, 56.47 and 82.27 percent for GLONASS, respectively.

With the static results in table 2, we can also compute the average accuracy of yaw, pitch and roll for each GNSS system on August 22. Since the accuracy in the last three rows of static data (namely, 30, 40 and 50 min in the first part of precise relative positioning) may likely indicate slight motion of the platform, as explained in the end of section 3.1, it is not included in the average computation. In general, as in the case of March 22, the baseline-based static attitude solutions are much better than that of the dynamical ones. More precisely, the average

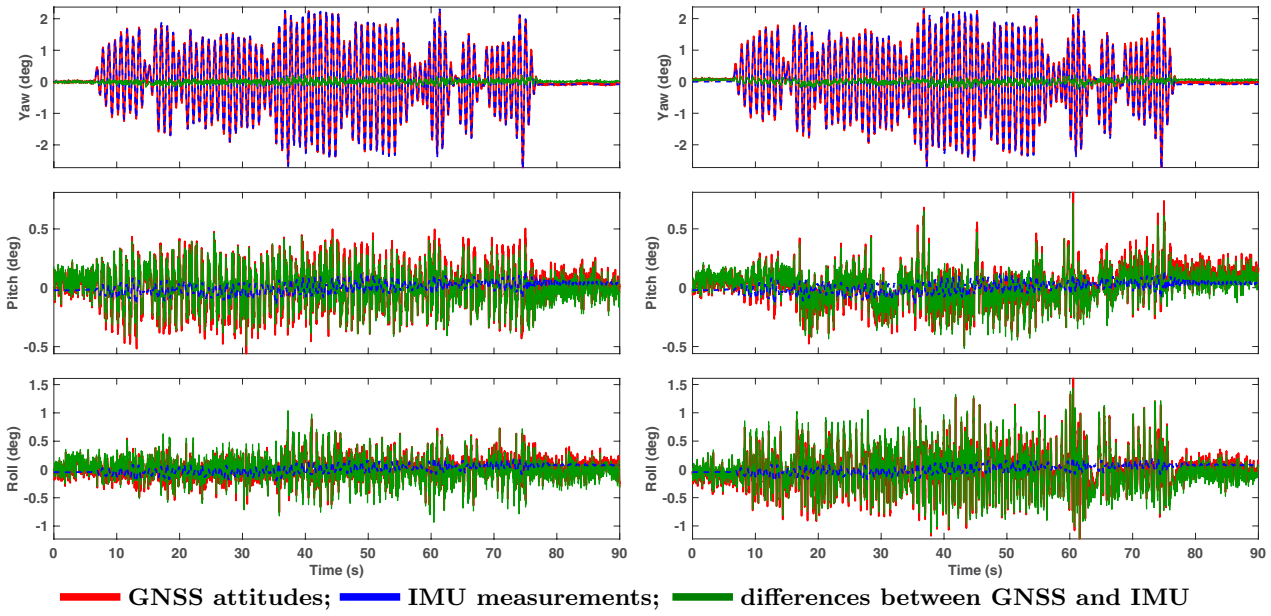

Figure 7. The high-rate, baseline-based GPS and GLONASS dynamical attitude solutions determined from GPS and GLONASS baselines, together with the IMU measurements for the platform during the first dynamical experiment on March 22. The GPS and GLONASS high-rate attitude solutions are shown in the left and right panels, respectively.

accuracy of the static experiments over the dynamical experiments on August 22 is now about 2.33, 1.14 and 1.15 times better in yaw, pitch and roll for GPS, 1.04, 1.06 and 1.50 times better for Beidou, 0.58, 0.20 and 0.35 times better for GLONASS, respectively. GPS performs slightly better than GLONASS in both yaw and roll, but among three of the four dynamical experiments, GLONASS shows a bit better than GPS in pitch, which can also be observed in the experiments of March 22.

Since the four independent high-rate GNSS dynamical attitude experiments on March 22 show more or less a similar error nature, we plot the high-rate baseline-based GPS and GLONASS attitude solutions during the first dynamical experiment in figure 7, together with the IMU attitude solutions. Figure 7 has shown that when compared with the IMU attitude results, the yaw components are consistently of the least errors for both GPS and GLONASS, followed by the pitch components, as numerically confirmed by the above analysis of statistics in table 4. The roll components are of the worst performances. This observation of errors between GNSS and IMU can also be readily confirmed numerically by the accuracy results listed in columns 'roll' below precise relative positioning in table 4. A careful look at the subplots of pitch and roll components in figure 7 reveals that in the first dynamical experiment on March 22 with the yaw direction set in motion, the high-rate dynamical attitude solutions in the pitch and roll directions are significantly different from the corresponding IMU measurements. The same phenomena of poor determination of the roll angles have been consistently observed in the other three dynamical experiments as well but not shown here.

There may be three possible reasons to explain the phenomenon of significant differences between the high-rate GNSS attitude solutions and the IMU measurements in the pitch direction, and in particular, the roll direction. As the first possible reason, we recall that the three Trimble Net R9 antennas (Ant1, Ant2 and Ant3) are installed on two almost orthogonal aluminium bars, as described and illustrated in the experimental design (compare figure 1). Since the bars are of a rectangular size of 8.44 cm (horizontal) and 4.90 cm (vertical) and because of the weights of the antennas, the bars could be subject to vertical flexure during the dynamical experiments to some extent, in particular, if the vertical motions are involved. As a likely result of the aluminium bars, this configuration of antennas may favor more on the yaw measurements of the platform and better match the IMU yaw outputs on the platform than the other two measurements of pitch and roll. The flexures of aluminium bars may result in extra pitch and roll values during a dynamical experiment, which should be zero in the case of static experiments. However, the IMU has been firmly installed on a rigid plate and should certainly not contain any information on pitch and roll motions due to the flexures of aluminium bars and the weights of antennas. This may explain the small values of the IMU-measured rolls and the significant errors of the GPS and GLONASS rolls when compared with the IMU measurements. Second, as is

Table 6. The standard deviations (mm) of the baselines with each of the multi-GNSS systems during the static experiments on March 22. Baseline 1 refers to Ant1 and Ant2, and Baseline 2 to Ant1 and Ant3. multi-GNSS refers to the combined multi-GNSS constellation of GPS, Beidou and GLONASS.

	Baseline 1			Baseline 2		
Systems	East	North	Up	East	North	Up
GPS	1.9	3.2	5.5	2.0	2.6	7.4
Beidou	2.1	2.5	7.8	3.5	3.4	11.8
GLONASS	3.3	1.7	8.5	4.7	2.2	10.0
Multi-GNSS	1.2	1.3	4.0	1.7	1.4	4.3

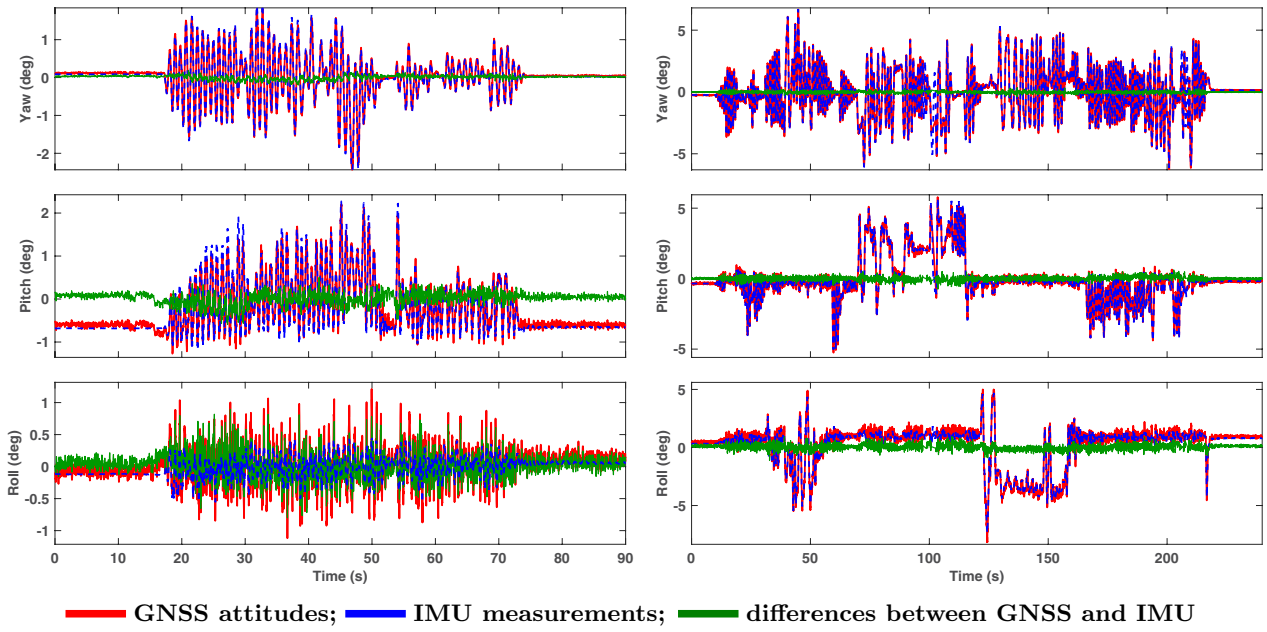

Figure 8. The high-rate multi-GNSS attitude solutions determined from precise multi-GNSS baselines and the IMU measurements for the platforms during the fourth dynamical experiments on both March 22 (left panel) and August 22 (right panel).

well known, the accuracy of the vertical component in precise relative positioning is usually 2–4 times worse than that of the horizontal components. This is also the case with our experiments, as is confirmed in table 6, which lists the standard deviations of the baselines during the first 3000 s of static period in the experiments on March 22. Since yaw is affected by the horizontal components of the baselines, it should be of the best possible accuracy (Lu *et al* 1994). However, because both pitch and roll are directly involved with the vertical component, their accuracy will be readily affected by the poor accuracy of the vertical components of the baselines. As the last possible reason to explain the large errors of pitch, and in particular, roll components, we may mention that the baseline projected along the roll direction is shorter (compare figure 1). Thus, the corresponding accuracy of rolls can be theoretically expected to be poorer.

To give the reader an impression of the combined multi-GNSS attitude determination, we show the final multi-GNSS attitude solutions of the fourth dynamical experiment on both March 22 and August 22 in figure 8, together with the IMU attitude measurements. We can also clearly see from figure 8 that the yaw component is best determined by the multi-GNSS constellation, followed by the pitch component. The roll component is reconstructed with the largest uncertainty.

3.3. High-rate multi-GNSS PPP attitude determination and comparison with IMU

Although conventional PPP is generally of accuracy at the level of centimeters in the long term (of say, hours to months) (Kouba 2003, Bahadur and Nohutcu 2018, Liu *et al* 2018, figure 8), high-rate GNSS PPP has been shown to enable to achieve the 2–4 mm accuracy of positioning over a short period of time, which is comparable with that of precise relative positioning of short baselines through exact GNSS ambiguity resolution. The reason for the high accuracy of PPP over a short period of time is that most of random errors in the long term can be treated as systematic errors within a short period of time and can be almost completely removed or substantially reduced, as experimentally demonstrated in Xu *et al* (2013) (see also Yigit (2016)) and systematically analyzed by Shu *et al* (2017). Paziewski *et al* (2018) recently also demonstrated a millimetre level of accuracy of high-rate RTK and PPP with a multi-GNSS constellation. As part of the experiments in this paper, we would like to apply high-rate multi-GNSS PPP to determine attitudes over a short period of time and investigate what accuracy PPP-based high-rate attitude solutions can achieve. More precisely, we will first compute the high-rate PPP positions of the three antennas over a short period of time, turn these positions into the baselines or vectors between the antennas and then apply the optimization model (2) to determine the PPP-based attitude solutions. We have used the procedures described in Xu *et al* (2013) to determine the scaling factors and timing misalignments with the waveforms of GNSS relative positioning and the two IMUs. Since precise relative positioning is more precise for very short baselines than PPP, we will directly use the scaling factors and timing misalignment in section 3.2 to correct the IMU measurements before the PPP-based high-rate attitude solutions are compared with the IMU measurements.

As in Xu *et al* (2013), we use the software system PANDA to compute PPP solutions of the three antennas with convergent floating ambiguities in its current version. The basic observational equations are ionosphere-free combinations of dual frequency P-code and carrier phase observables on the basis of GPS L1 and L2, Beidou B1 and B2, GLONASS L1 and L2, and Galileo E1 and E5a frequencies. The following elevation-dependent function is used to determine the weights of ionosphere-free observables:

$$w(A_e) = \begin{cases} 1, & \text{if } A_e > 30^\circ \\ 2\sin(A_e), & \text{if } A_e \leqslant 30^\circ, \end{cases} \quad (3)$$

where A_e is the elevation angle. The PCO/PCV models by Schmid *et al* (2016) are used to correct antenna phase centers. Tidal effects are corrected after the IERS conventions 2003 and the Saastamoinen model is used to correct tropospheric delays. The PANDA software system detects cycle slips of carrier phase observables by using the geometry-free combination, Melbourne–Wübbena combination, the ionosphere-free combination and the loss of lock indicator. The MGEX products are provided by Wuhan University, which include precise orbit and clock products (Guo *et al* 2015). In the case of GPS, the IGS final precise orbit and 5s satellite clock products are directly used in the experiments on March 22 and August 22. However, due to a limited available distribution of tracking stations, we can only use the 300s satellite clock and 15 min orbit products for the other GNSS systems (http://mgex.igs.org/IGS_MGEX_Products.php), since the experiments were actually conducted in 2014. The unknown parameters to be estimated include epoch-wise station coordinates, epoch-wise receiver clock errors and residual zenith total delays for a pre-determined length of arc (say 2 h). The cutoff angle in the following experiments is set to 10 degrees and the convergence time in our PPP processing is about 20–40 min. For more technical details on PANDA and its application to high-rate PPP solutions, the reader is referred to Liu and Ge (2003) and Xu *et al* (2013).

Based on the high-rate PPP positions of the three antennas fixed to the motionless platform, we have computed the high-rate PPP-based static attitude solutions. As a result, we can further compute the standard deviations of the three attitude angles with the static data of 1, 3, 5, 10, 20, 30, 40 and 50 min, respectively, which have been listed in table 1 for the experiments on March 22 and table 2 for the experiments on August 22, respectively. Some general features of the high-rate PPP-based attitude solutions can be clearly observed from tables 1 and 2:

(i) the high-rate PPP-based attitude solutions are consistently worse in accuracy than the baseline-based attitude solutions after the correct ambiguity resolution for each of the multi-GNSS systems on both days of experiments. The baseline-based attitude solutions are, on average, about 1.23, 2.59 and 1.85 times better than the PPP-based attitude solutions for GPS, 2.01, 1.44 and 1.32 times better for Beidou, and 4.87, 4.83 and 4.34 times better for GLONASS, respectively, as computed from the static part of the experiments in table 1 on March 22. Such improvements are smaller for the experiments on August 22 but not reported here in details;

(ii) unlike the baseline-based attitude solutions, the PPP-based attitude solutions tend to significantly degrade in accuracy with the increase of time in the short term (of say, up to 1 h), which is more or less consistent with the general behavior of accuracy degradation of PPP coordinate solutions. As explained in Xu *et al* (2013), within a short period of time, except for the noises of measurements, almost all other errors such as multipath, troposphere and ionosphere are of systematic nature and can be cancelled out by time difference. With the increase of time, residual errors of systematic sources tend to behave randomly. As a result, the corresponding standard deviations of PPP solutions become larger with time in the short term. Nevertheless, after some certain time, the randomness of residual errors may remain stable and so are the error levels of the corresponding PPP solutions in the long term;

(iii) to compare the PPP-based attitude solutions with the static data, in general, GPS has the best accuracy performance, followed by Beidou. GLONASS performs the worst in the PPP-based attitude solutions. If limited to a short period of time up to 5 min with the static data on March 22, on average, GPS can be 1.28, 0.48 and 0.75 times better than Beidou in yaw, pitch and roll, and 2.01, 0.69 and 0.61 times better than GLONASS, respectively. On average, Beidou performs slightly better than GLONASS in yaw and pitch by 32.20 and 14.60 percent, respectively but slightly worse in roll by 10.10 percent. In the case of the static experiments on August 22, although GPS performs even much better than Beidou and GLONASS, Beidou is now negligibly worse than GLONASS in yaw but much better in pitch and roll by a factor of 0.17 and 1.29 times, respectively; and finally,

(iv) the PPP-based yaw solutions look quite well and stable within a short period of time up to 5 min, which likely reflects the fact that PPP positionings in the horizontal components are much better than that in the vertical component. Within such a short time span, the GPS baseline-based yaw solutions are only better than the PPP-based yaw solutions, on average, by a factor of 86.49 percent on March 22 (compare table 1) and 69.62 percent on August 22 (compare table 2), respectively. In the case of Beidou and GLONASS, such an improvement rate can reach a factor of 3.23 times in roll for the experiments on March 22. Actually, within a short period of time up to 3 min, the combined high-rate PPP-based attitude solutions with the multi-GNSS constellation in the static experiments seem to be even better than the baseline-based attitude solutions in the dynamical experiments, as may be inferred by comparing the accuracy in the first three lines of column 'multi-GNSS' below *precise point positioning* in table 1 with that in the four lines of column 'GPS' below *precise relative positioning* in table 4. In other words, within a short period of time, static PPP-based attitude solutions can perform better than dynamical baseline-based solutions. This observation also applies to the experiments on August 22.

We will now focus on dynamical experiments. More precisely, we will investigate the performances of high-rate PPP-based attitude solutions, in particular, within a short period of time, and compare them with the IMU measurements in the dynamical experiments on both March 22 and August 22. Due to the space limit, we show the first two dynamical experiments on

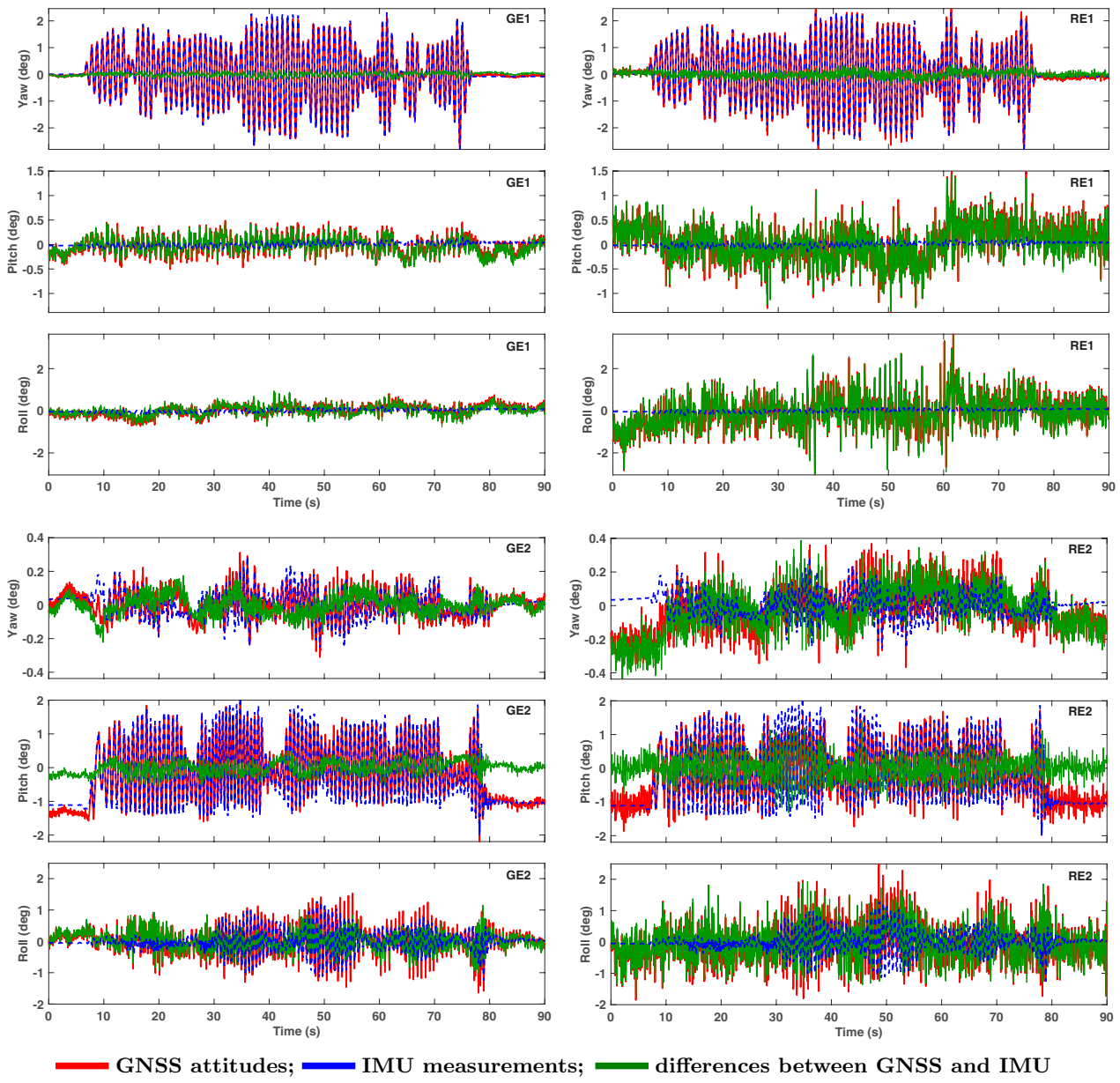

Figure 9. The high-rate PPP-based attitude solutions, the IMU measurements for the platform and their comparisons of the first two dynamical experiments on March 22. The GPS PPP and GLONASS PPP attitude solutions are shown on the left and right panels, respectively. The upper and lower three panels report the results of the first and second dynamical experiments, respectively.

March 22 to illustrate the performances of the high-rate PPP-based attitude solutions. The high-rate attitude solutions of these two dynamical experiments with GPS and GLONASS are respectively shown in the left and right panels of figure 9, together with the corresponding IMU measurements. It is clear after a quick comparison of the left and right panels in figure 9 that the widths of all the green lines on the left are smaller than those on the right, indicating that the GPS PPP-based attitude solutions are all much better determined than the corresponding GLONASS solutions. Actually, if we compare the accuracy results in columns 'GPS' and 'GLONASS' below *precise point positioning* in table 4, we find that, on average, the accuracy of the GPS PPP-based attitude solutions is much better than that of GLONASS by a factor of 0.32–1.38 times in yaw, 0.75–2.72 times in pitch, and 0.71–2.22 times in roll, respectively. The average improvement rates with the four dynamical experiments are equal to 0.76, 1.40 and 1.19 times in yaw, pitch and roll, respectively. Although the multi-GNSS baseline-based attitude solutions without Beidou are obviously better than those with Beidou in the experiments on March 22, there is no clear winner in these four dynamical PPP-based experiments, as can be seen from the PPP results in table 4. The combined PPP-based solutions with GPS and GLONASS are clearly better than those with GLONASS only by an average value of 58.21, 109.29 and 82.01 percent in yaw, pitch and roll, respectively. However, they are slightly worse than those with GPS only by comparing the PPP-based results in columns 'GPS' and 'GPS + GLONASS', with an average factor of 7.27, 10.95 and 15.01 percent in yaw, pitch and roll, respectively; the results are a bit surprising and may

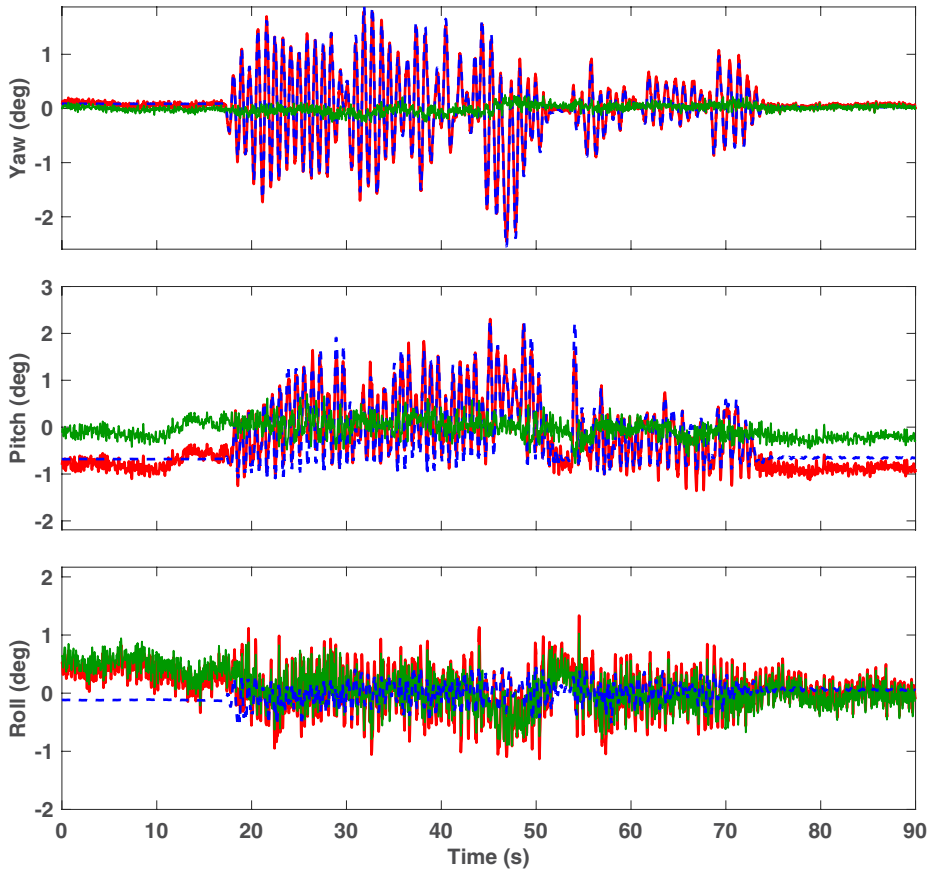

Figure 10. The high-rate multi-GNSS PPP-based attitude solutions and the IMU measurements for the platform of the fourth dynamical experiment on March 22. Red lines—multi-GNSS PPP-based attitude solutions without Beidou; blue lines—IMU attitude measurements; green lines—the differences of multi-GNSS PPP-based attitudes from the IMU measurements.

again strongly imply the importance of properly incorporating variance component estimation to combine different GNSS systems. To illustrate the performance of the combined multi-GNSS PPP-based attitude solutions, we show the attitude solutions of the fourth dynamical experiment on March 22 in figure 10, together with the IMU measurements.

As in the case of baseline-based attitude determination in section 3.2, we can also clearly see from figure 9 that the errors of PPP-based pitch and roll solutions are either much larger (compare the pitch and roll components in the top three panels) or at least, comparable with the IMU measurements in the case of the roll component (compare the bottom two panels). The three possible reasons for large errors in pitch and roll may still well apply here, namely, the flexure of the aluminium bars due to the dynamical motion and the weights of antennas, the large errors in the vertical component of precise GNSS positioning and a shorter baseline projected along the roll direction, as explained in section 3.2.

Since there was no problem in locking on Beidou satellites on August 22, we will now further show the PPP-based attitude results of the dynamical experiments. The corresponding accuracy statistics are also listed in table 5. Table 5 shows that all the multi-GNSS systems have the best performance in determining the yaw angle. The multi-GNSS constellation basically performs better than any single GNSS system, as can be seen from the PPP-based accuracy results in table 5. Nevertheless, if we compare the accuracy of pitch from the multi-GNSS constellation in the third and fourth dynamical experiments with that from GPS, we can again see the importance and necessity of incorporating variance component estimation in the multi-GNSS constellation, which should be investigated in the future.

In general, the GPS PPP-based attitude solutions significantly outperform those with Beidou and GLONASS in all the four dynamical experiments on August 22 (compare table 5). More precisely, the accuracy of GPS PPP-based results is significantly better than that of Beidou by a factor of 0.34–0.77 times in yaw, with an average value of 0.53 time, a factor of 0.96–2.65 times in pitch, with an average value of 1.88 times, and a factor of 2.06–6.81 times in roll, with an average value of 3.49 times, respectively. When compared with GLONASS, the accuracy of GPS PPP-based results is better by a maximum percentage of 77.40 for the first three dynamical experiments but significantly better in the fourth experiment by a factor of 1.75, 2.46 and 1.39 times in yaw, pitch and roll, respectively. When comparing the accuracy results of Beidou with those of GLONASS, we can see that Beidou performs slightly better than GLONASS in yaw but significantly worse by a factor of 1.04 and 2.23 times in pitch and roll, respectively.

To give the reader an impression on the general performances of each of the GNSS systems and the combined

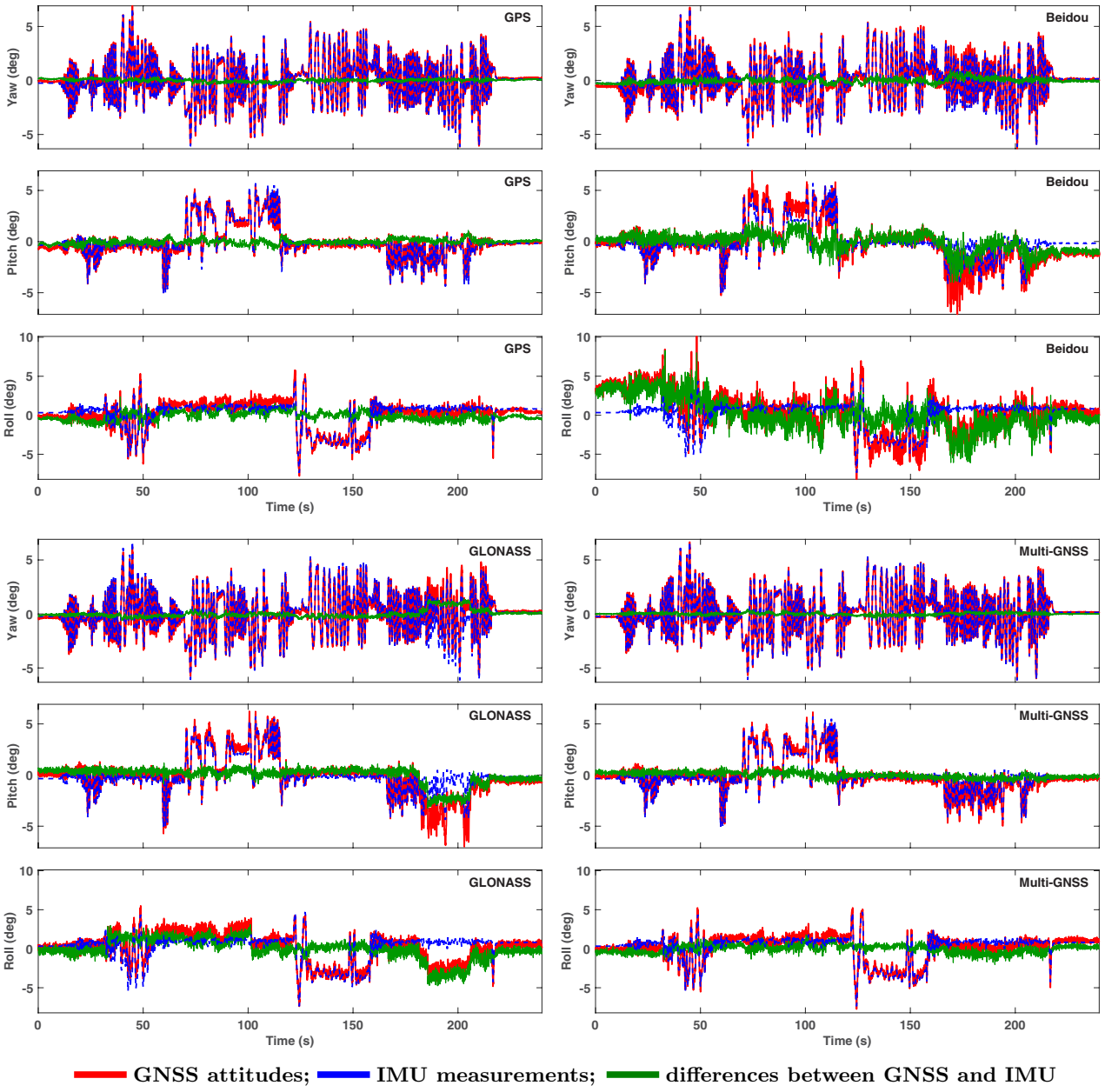

Figure 11. The high-rate PPP-based attitude solutions and the IMU measurements of the platform for the fourth dynamical experiment on August 22. GPS PPP—upper-left three panels; Beidou PPP—upper-right three panels; GLONASS PPP—lower-left three panels; multi-GNSS PPP—lower-right three panels. In the multi-GNSS PPP-based attitude solutions, two Galileo satellites are also included together with GPS, Beidou and GLONASS.

multi-GNSS constellation, we show the high-rate PPP-based attitude solutions of the fourth dynamical experiment on August 22 in figure 11, together with the corresponding IMU measurements.

4. Dynamical rotations from the GEONET stations during the 2011 Tohoku Mw 9.0 earthquake

Rotational seismology has been a recent topic of great interest in seismology, thanks to tremendous advance in modern technology of measurement (Igel *et al* 2007, Lee *et al* 2007, 2009, Pillet and Virieux 2007, Graizer 2009a). Four international workshops have regularly been devoted to rotational seismology, since the first workshop was held at the U.S. Geological Survey, Menlo Park in 2007. For more information on rotational seismology, the reader may refer to Lee *et al* (2007) and the web site www.rotational-seismology.org/ managed by the international working group on rotational seismology. Although rotational motion was believed to not exist and was not actually observed more than a century ago, Reid (1910) mentioned that small rotational motions could theoretically be possible. Damage reports of earthquakes documented in the historical literature of large earthquakes may imply that such motions could be real, as shown with evidence by the rotational shifts or destructions of vertically placed structures such as chimneys and grave tombstones (Lee *et al* 2007, 2009, Kozák 2009), though a mechanical interpretation

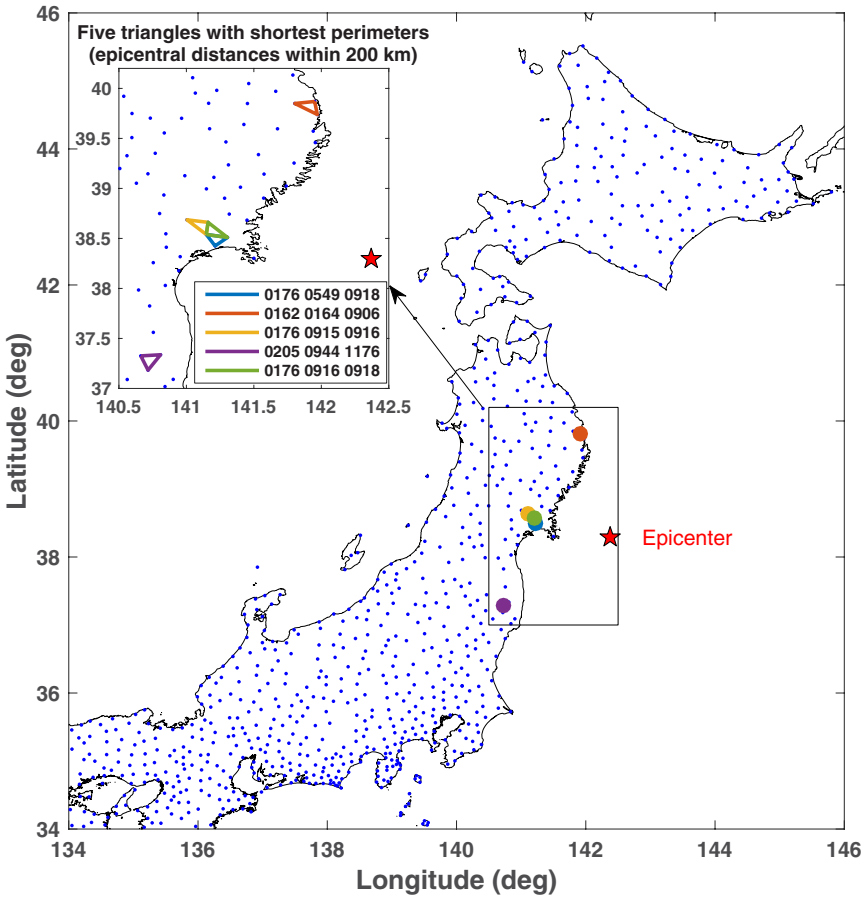

Figure 12. The hypocenter of the 2011 Tohoku Mw9.0 earthquake and the locations of five GPS triangles (marked in different colors with the station codes) used to compute the rotational motions.

of such observed rotations can be possible. Recent measurement evidences with high precision gyros can be found, for example, in Igel *et al* (2007), Pillet and Virieux (2007) and Graizer (2009a).

Since rotational motions due to large earthquakes are small (Reid 1910) and cannot be measured with conventional seismometers without attitude information, some recent measurements and theoretical research have shown that rotations due to earthquakes can reach some arc minutes (Niazi 1986, Takeo 2009) and tilts can be in the order of a few degrees (Graizer 2009b). With the modern advance of GNSS technology, it is likely reasonable at the present stage to detect such small rotations and tilts by using a proper configuration of GNSS antennas with sufficient confidence. If a configuration of GNSS antennas is sufficiently large, the accuracy of measuring a rotational motion with GNSS can be very high. For example, assuming 10 km for baselines with an accuracy of 5 mm, we could roughly expect that this high precision GNSS configuration can detect a rotational motion of 0.2 arc second with a confidence of 95 percent. Based on multi-GNSS constellations, a short baseline of up to 50 m with an accuracy of 1–2 mm should not be a problem technically and the corresponding rigid GNSS antenna configuration would be able to detect a rotation at the best possible accuracy of about 4.1 arc seconds. As a result, multi-GNSS rotational seismology should be technologically realistic to measure a few arc seconds level of rotational motions with a large confidence in the future, not to mention that a properly designed rigid configuration of GNSS antennas with a mean baseline up to 100 m should probably not be difficult technically either.

Nevertheless, because no GNSS antennas have been purposely installed to detect seismological rotations and because GNSS antennas currently applied in earth sciences are not rigidly connected together on the surface of the Earth, a current configuration of GNSS antennas would likely detect a mixture of small rotational motions and seismic wave motions passing through the points where antennas are installed. Even being well aware of this fact of mixed phenomena, we would take the 2011 Tohoku Mw9.0 earthquake as an example and make an attempt to compute the rotational motions with the GNSS data of GEONET. At the very least, this preliminary analysis can be qualitatively constructive, since none of conventional seismometers can be used to measure rotational motions of earthquakes, unless they are rigidly fixed together.

For this rotatory analysis, we have carefully selected some GEONET stations, which are sufficiently close together to form a GNSS configuration of attitude determination with shortest possible baselines and meanwhile are as close as possible to the hypocenter of the 2011 Tohoku Mw9.0 earthquake. As a result, we select five GNSS triangles, which are shown in figure 12, together with the Tohoku Mw9.0 hypocenter. The average length of the sides of each triangle is equal to 13.4,

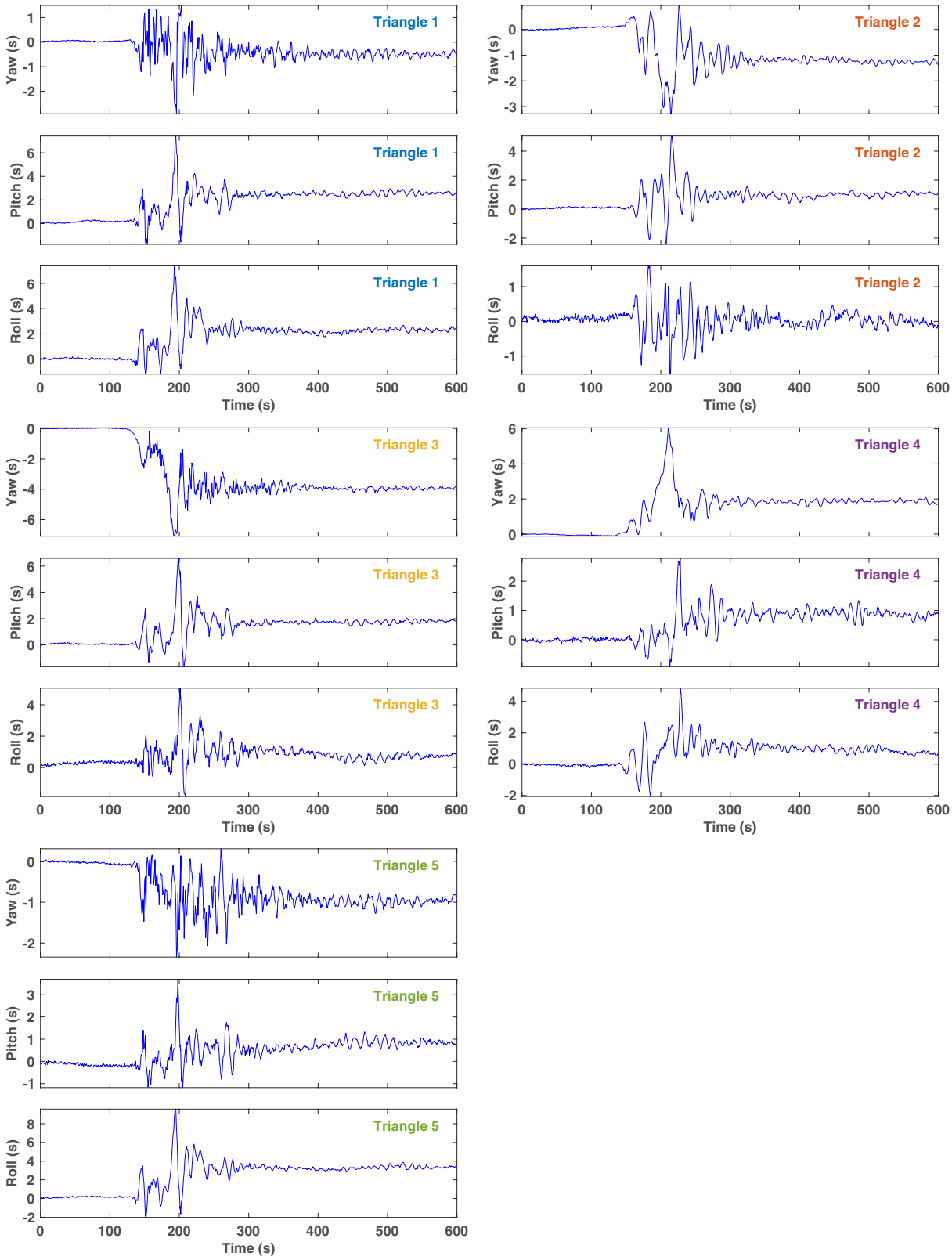

Figure 13. The baseline-based dynamical rotational motions of the five GPS triangles during the 2011 Tohoku Mw9.0 earthquake. The triangles 1–5 refer to the upper-left three panels, the upper-right three panels, the middle-left three panels, the middle-right three panels, and the lower-left three panels, respectively.

15.4, 16.0, 16.2 and 16.2 km, respectively. We have applied the baseline-based method to determine the attitudes of the antenna configurations. The rotational waveforms have been shown in figure 13. The coseismic rotations and the amplitudes of rotations during the earthquake are summarized in table 7. The three triangles closest to the hypocenter, namely, triangles 1, 3 and 5 in table 7, are subject to the largest coseismic rotations and the largest amplitudes of rotations, with a maximum

Table 7. The coseismic rotations and the amplitudes of rotations during the earthquake for the five triangles shown in figure 12 (units: seconds).

	Coseismic rotations			Amplitudes		
Triangles	Yaw	Pitch	Roll	Yaw	Pitch	Roll
Triangle 1	−0.54	2.44	2.32	4.41	9.19	8.58
Triangle 2	−1.31	0.90	−0.06	4.22	7.48	3.12
Triangle 3	−3.96	1.72	0.42	6.95	8.24	6.91
Triangle 4	1.94	0.89	0.95	6.18	3.69	6.91
Triangle 5	−0.95	0.98	3.24	2.65	4.87	11.58

coseismic value of −3.96 arc seconds in the yaw direction of triangle 3 and a maximum amplitude of 11.58 arc seconds in the roll direction of triangle 5.

It is interesting to find that the negative yaw values of four triangles in the northern part of the hypocenter indicate that the 2011 Tohoku Mw9.0 earthquake triggered this northern area to rotate anti-clockwise and the yaw value in triangle 4 in the south shows that this area with triangle 4 rotates clockwise. This pattern of rotatory motions in yaw may be physically interpreted as that the Sendai area with triangles 1, 3 and 5 has been most pulled towards the hypocenter. Except for a very small negative roll value in triangle 2, all the other rotatory motions around pitch and roll are directionally consistent, implying that the Tohoku area inclines towards the Pacific and the south. We should note, however, that since all the five triangles are certainly not rigid, the reported seismic rotations in table 7 should probably be a mixture of seismic rotatory and earthquake wave motions. Nevertheless, the rotatory results demonstrate the potential of multi-GNSS to detect rotatory seismic motions, if a sufficient large configuration of GNSS antennas is properly installed, for example, on the basis of some integrated building complex.

5. Concluding remarks

High-rate GNSS relative positioning has been widely applied to problems in sports (Buchheit *et al* 2014, Hoppe *et al* 2018), earth sciences (Kouba 2003, Larson *et al* 2003, Genrich and Bock 2006, Grapenthin and Freymueller 2011, Xu *et al* 2013) and civil engineering (Lovse *et al* 1995, Psimoulis *et al* 2008, Moschas and Stiros 2011, 2014, 2015, Im *et al* 2013, Kaloop and Kim 2014, Roberts and Tang 2017). We have extended high-rate GNSS positioning to high-rate GNSS attitude determination with particular attention to the current state-of-the-art multi-GNSS systems. A series of experiments of high-rate GNSS attitude determination were conducted on a platform with three 50 Hz geodetic GNSS receivers and high-grade inertial measurement units (IMU) on March 22, 2014 and August 22, 2014. Generally speaking, the experimental results on these two days have clearly shown that the high-rate GPS attitude results are of the best accuracy, followed by GLONASS. The high-rate Beidou attitude results are generally the noisiest.

As the first part of experiments, we have used the double-difference observational model of carrier phases, fixed the integer ambiguities, computed the precise baselines and then determined the high-rate multi-GNSS attitude solutions. Both the static and dynamical experiments through the comparison with the zero true values and/or the IMU measurements have confirmed that the baseline-based method is applicable to precisely determine the high-rate multi-GNSS attitudes of the platform for each GNSS system alone and its accuracy remains quite stable with time. The high-rate baseline-based GNSS attitude solutions have also shown that yaw can be best determined. But pitch and roll are much noisier, due to the well-known poor accuracy of GNSS positioning in the vertical component and our experimental settings. The combined multi-GNSS constellation can generally significantly improve the high-rate GNSS attitude solutions, in particular, in the case of static experiments with an accuracy of 0.01–0.02 degrees for a configuration with an average baseline of about 3–5 m. Multi-GNSS attitude determination can outperform any single GNSS system to detect rotational motion for any platform in slow or quasi-static motion. The high-rate baseline-based attitude solutions in the dynamical experiments are significantly less accurate than those in the static experiments. In some cases, the experimental attitude solutions have also clearly shown that the multi-GNSS constellation may perform slightly worse than GPS in some components in the dynamical experiments, which may likely be due to improper weightings of carrier phase measurements from different GNSS systems.

We have attempted to apply the PPP-based method to determine high-rate attitude solutions under the framework of the multi-GNSS systems. Within a short period of time, PPP-based high-rate attitude solutions with the combined multi-GNSS constellation of GPS, Beidou, GLONASS and Galileo are shown to enable to achieve almost the comparable level of accuracy of baseline-based attitude solutions from any single GNSS system in the dynamical experiments. The high-rate PPP-based pitch and roll solutions perform much worse than the corresponding yaw solutions, which should theoretically be consistent with the general performance of high-rate PPP positioning, since they are involved with the less accurate vertical component of GNSS positioning. The yaw solutions can further be significantly improved with the combined multi-GNSS constellation. The poor performances of the PPP-based pitch and roll solutions may again be attributed to the relatively poor accuracy of high-rate PPP positioning in the vertical direction and our experimental settings. The experimental results have clearly demonstrated that the accuracy of high-rate PPP-based attitude solutions substantially degrades with time.

The high-rate attitude solutions from both the static and dynamical experiments have shown that baseline- and PPP-based methods are capable of determining high-rate attitudes and precisely measuring rotatory motions within a short period of time. As an application example of high-rate GNSS attitude determination in rotational seismology, we analyze the GEONET data of the 2011 Tohoku Mw9.0 earthquake,

even though we are well aware of the fact that the rotatory motions are a mixture of both seismic rotatory and wave motions. The rotatory results have clearly demonstrated the potential of using a multi-GNSS constellation to precisely measure seismic rotatory motions. Actually, the accuracy of the high-rate multi-GNSS static attitude solutions from our experiments can be as high as 0.01 degrees or equivalently 1.7×10^{-4} rad, which is sufficient to precisely detect any rotatory motion induced by earthquakes larger than M5.0 (Takeo 2009). The multi-GNSS baseline solutions in the horizontal components have also been shown to readily reach the accuracy of 1 mm. If a configuration of multi-GNSS antennas is of an average 50 m baseline, the yaw accuracy is expected to reach about 4 arc-seconds, which can easily detect rotatory motions due to large earthquakes with a high confidence.

Finally, we may like to note that since an attitude determination configuration contains more information than a naive PPP, the PPP-based method of attitude determination could be theoretically further improved and more work should be done along this direction. The static and dynamical experiments have clearly shown that variance component estimation should also be incorporated in multi-GNSS attitude determination, which should be further investigated. Applications in engineering structures should be highly expected in the future.

Acknowledgments

We thank Dr Quan Zhang for his kind help and support in the beginning of this work. We also thank the three anonymous reviewers for their very detailed and very constructive comments, which have helped significantly improve and clarify parts of this paper. This work is partially supported by the National Natural Science Foundation of China (projects No. 41231174, No. 41674013 and No. 41874012).

ORCID iDs

Peiliang Xu https://orcid.org/0000-0003-1830-8401

References

Ardalan A A and Rezvani M 2015 An iterative method for attitude determination based on misaligned GNSS baselines *IEEE Trans. Aerosp. Electron. Syst.* **51** 97–106

Arun K S, Huang T S and Blostein S D 1987 Least-squares fitting of two 3d point sets *IEEE Trans. Pattern Anal. Mach. Intell.* **9** 698–700

Bahadur B and Nohutcu M 2018 PPPH: a MATLAB-based software for multi-GNSS precise point positioning analysis *GPS Solut.* **22** UNSP 113

Baksalary J K 1984 A study of the equivalence between a Gauss–Markoff model and its augmentation by nuisance parameters *Math. Oper.forsch. Stat. Ser. Stat.* **15** 3–35

Bischof C and Schön S 2017 Vibration detection with 100 Hz GPS PVAT during a dynamic flight *Adv. Space Res.* **59** 2779–93

Black H D 1964 A passive system for determining the attitude of a satellite *AIAA J.* **2** 1350–1

Bock Y, Melgar D and Crowell B W 2011 Real-time strong-motion broadband displacements from collocated GPS and accelerometers *Bull. Seismol. Soc. Am.* **101** 2904–25

Buchheit M, Haddad H A, Simpson B M, Palazzi D, Bourdon P C, Salvo V D and Mendez-Villanueva A 2014 Monitoring accelerations with GPS in football: time to slow down? *Int. J. Sports Physiol. Perform.* **9** 442–5

Cannon M E and Sun H 1996 Experimental assessment of a non-dedicated GPS receiver system for airborne attitude determination *ISPRS J. Photogramm. Remote Sens.* **51** 99–108

Chang X W, Yang X and Zhou T 2005 MLAMBDA: a modified LAMBDA method for integer least squares estimation *J. Geod.* **79** 552–65

Cohen C E 1992 Attitude determination using GPS: development of an all solid-state guidance, navigation, and control sensor for air and space vehicles based on the global positioning system *PhD Thesis* Stanford University

Cohen C E 1996 Attitude determination *Global Positioning System: Theory and Applications* vol II, ed B W Parkinson and J J Spilker Jr (Washington, DC: American Institute of Aeronautics and Astronautics) pp 519–38

Cohen C E, McNally B D and Parkinson B W 1993 Flight tests of attitude determination using GPS compared against an inertial navigation unit *Presented at the ION National Technical Meeting (San Francisco, CA, 20–22 January 1993)*

Crassidis J L, Markley F L and Cheng Y 2007 Survey of nonlinear attitude estimation methods *J. Guid. Control Dyn.* **30** 12–28

Davenport P B 1968 A vector approach to the algebra of rotations with applications *NASA Technical Note TN* D4696

Ellis J F and Creswell J A 1979 Interferometric attitude determination with the global positioning system *J. Guid. Control* **2** 522–7

Evans A G 1986 Roll, pitch, and yaw determination using a global positioning system receiver and an antenna periodically moving in a plane *Mar. Geod.* **10** 43–52

Farrell J L and Stuelpnagel J C 1966 A least squares estimate of satellite attitude (Grace Wahba) *SIAM Rev.* **8** 384–6

Fincke U and Pohst M 1985 Improved methods for calculating vectors of short length in a lattice, including a complexity analysis *Math. Comput.* **44** 463–71

Gebre-Egziabher D, Hayward R C and Powell J D 2004 Design of multi-sensor attitude determination systems *IEEE Trans. Aerosp. Electron. Syst.* **40** 627–49

Genrich J F and Bock Y 2006 Instantaneous geodetic positioning with 10–50 Hz GPS measurements: noise characteristics and implications for monitoring networks *J. Geophys. Res.* **111** B03403

Graizer V 2009a Tutorial on measuring rotations using multipendulum systems *Bull. Seismol. Soc. Am.* **99** 1064–72

Graizer V 2009b Tilts in strong ground motion *Bull. Seismol. Soc. Am.* **99** 2090–102

Grapenthin R and Freymueller J T 2011 The dynamics of a seismic wave field: animation and analysis of kinematic GPS data recorded during the 2011 Tohoku-oki earthquake, Japan *Geophys. Res. Lett.* **38** L18308

Grewal M S, Weill L R and Andrews A P 2001 *Global Positioning Systems, Inertial Navigation and Integration* (New York: Wiley)

Gross J N, Gu Y, Rhudy M B, Gururajan S and Napolitano M R 2012a Flight-test evaluation of sensor fusion algorithms for attitude estimation *IEEE Trans. Aerosp. Electron. Syst.* **48** 2128–39

Guo J, Xu X, Zhao Q and Liu J 2015 Precise orbit determination for quad-constellation satellites at Wuhan University: strategy, result validation, and comparison *J. Geod.* **90** 143–59

Henkel P S 2015 Tightly coupled precise point positioning and attitude determination *IEEE Trans. Aerosp. Electron. Syst.* **51** 3182–97

Hofmann-Wellenhof B, Lichtenegger H and Collins J 1992 *GPS Theory and Practice* (New York: Springer)
Hoppe M W, Baumgart C, Polglaze T and Freiwald J 2018 Validity and reliability of GPS and LPS for measuring distances covered and sprint mechanical properties in team sports *PLoS One* **13** e0192708
Horn B, Hilden H M and Negahdripour S 1988 Closed-form solution of absolute orientation using orthonormal matrices *J. Opt. Soc. Am.* A **5** 1127–35
Igel H, Cochard A, Wassermann J, Flaws A, Schreiber U, Velikoseltsev A and Dinh N P 2007 Broad-band observations of earthquake-induced rotational ground motions *Geophys. J. Int.* **168** 182–96
Im S B, Hurlebaus S and Kang Y J 2013 Summary review of GPS technology for structural health monitoring *J. Struct. Eng.* **139** 1653–64
Juang J and Huang G 1997 Development of GPS-based attitude determination algorithms *IEEE Trans. Aerosp. Electron. Syst.* **33** 968–76
Kaloop M R and Kim D 2014 GPS-structural health monitoring of a long span bridge using neural network adaptive filter *Surv. Rev.* **46** 7–14
Kanatani K and Niitsuma H 2012 Optimal computation of 3D similarity: Gauss–Newton versus Gauss–Helmert *Comput. Stat. Data Anal.* **56** 4470–83
Keat J E 1977 Analysis of least-squares attitude determination routine DOAOP *Technical Report* CSC/TM-77/6034, Computer Sciences Corp., Maryland
Kijewski-Correa T, Kareem A and Kochly M 2006 Experimental verification and full-scale deployment of global positioning systems to monitor the dynamic response of tall buildings *J. Struct. Eng.* **132** 1242–53
Kouba J 2003 Measuring seismic waves induced by large earthquakes with GPS *Stud. Geophys. Geod.* **47** 741–55
Kozák J T 2009 Tutorial on earthquake rotational effects: historical examples *Bull. Seismol. Soc. Am.* **99** 998–1010
Lachapelle G, Cannon M E, Lu G and Loncarevic B 1996 Shipborne GPS attitude determination during MMST-93 *IEEE J. Ocean Eng.* **21** 100–5
Larson K M, Bodin P and Gomberg J 2003 Using 1 Hz GPS data to measure deformations caused by the Denali Fault earthquake *Science* **300** 1421–4
Lee W H K, Celebi M, Todorovska M I and Diggles M F 2007 Rotational seismology and engineering applications *Proc. 1st Int. Workshop (Menlo Park, CA, 18–19 September 2007)* p 46 (U.S. Geol Surv Open-File Report 2007-1144)
Lee W H K, Celebi M, Todorovska M I and Igel H 2009 Introduction to the special issue on rotational seismology and engineering applications *Bull. Seismol. Soc. Am.* **99** 945–57
Leite N P O and Walter F 2007 Flight test evaluation of a new GPS attitude determination algorithm *IEEE Aerosp. Electron. Syst. Mag.* **22** 3–10
Lenstra A K, Lenstra H W and Lovász L 1982 Factoring polynomials with rational coefficients *Math. Ann.* **261** 515–34
Liu J and Ge M 2003 PANDA software and its preliminary result of positioning and orbit determination *J. Nat. Sci. Wuhan Univ.* **8** 603–9
Liu T, Zhang B C, Yuan Y B and Li M 2018 Real-time precise point positioning (RTPPP) with raw observations and its application in real-time regional ionospheric VTEC modeling *J. Geod.* **92** 1267–83
Lovse J W, Teskey W F, Lachapelle G and Cannon M E 1995 Dynamic deformation monitoring of tall structure using GPS technology *J. Surv. Eng.* **121** 35–40
Lu G 1995 Development of a GPS multi-antenna system for attitude determination *PhD Thesis* Department of Geomatics Engineering, The University of Calgary
Lu G, Cannon M E and Lachapelle G 1994 Attitude determination using dedicated and nondedicated multiantenna GPS sensors *IEEE Trans. Aerosp. Electron. Syst.* **30** 1053–8
Markley F L 2002 Fast quaternion attitude estimation from two vector measurements *J. Guid. Control Dyn.* **25** 411–4
Markley F L and Mortari D 2000 Quaternion attitude estimation using vector observations *J. Astronaut. Sci.* **48** 359–80
Meng X, Dodson A H and Roberts G W 2007 Detecting bridge dynamics with GPS and triaxial accelerometers *Eng. Struct.* **29** 3178–84
Morrison A, Renaudin V, Bancroft J B and Lachapelle G 2012 Design and testing of a multi-sensor pedestrian location and navigation platform *Sensors* **12** 3720–38
Moschas F and Stiros S 2011 Measurement of the dynamic displacements and of the modal frequencies of a short-span pedestrian bridge using GPS and an accelerometer *Eng. Struct.* **33** 10–17
Moschas F and Stiros S 2014 Three-dimensional dynamic deflections and natural frequencies of a stiff footbridge based on measurements of collocated sensors *Struct. Control Health Monit.* **21** 23–42
Moschas F and Stiros S 2015 Dynamic deflections of a stiff footbridge using 100 Hz GNSS and accelerometer *J. Surv. Eng.* **141** 04015003
Niazi M 1986 Inferred displacements, velocities and rotations of a long rigid foundation located at El Centro differential array site during the 1979 Imperial Valley, California, earthquake *Earthq. Eng. Struct. Dyn.* **14** 531–42
Park F C, Kim J and Kee C 2000 Geometric descent algorithms for attitude determination using the global positioning system *J. Guid. Control Dyn.* **23** 26–33
Parkinson B W and Spilker J J Jr 1996 *Global Positioning System: Theory and Applications* (Washington, DC: American Institute of Aeronautics and Astronautics)
Paziewski J, Sieradzki R and Baryla R 2018 Multi-GNSS high-rate RTK, PPP and novel direct phase observation processing method: application to precise dynamic displacement detection *Meas. Sci. Technol.* **29** 035002
Pillet R and Virieux J 2007 The effects of seismic rotations on inertial sensors *Geophys. J. Int.* **171** 1314–23
Psimoulis P, Pytharouli S, Karambalis D and Stiros S 2008 Potential of global positioning system (GPS) to measure the frequencies of oscillations of engineering structures *J. Sound Vib.* **318** 606–23
Reid H F 1910 The California Earthquake of April 18, 1906 *The Mechanics of the Earthquake* (*Report of the State Earthquake Investigation Commission* vol 2) (Washington, DC: Carnegie Institution of Washington)
Roberts G W, Meng X L and Dodson A H 2004 Integrating a global positioning system and accelerometers to monitor the deflection of bridges *J. Surv. Eng.* **130** 65–72
Roberts G W and Tang X 2017 The use of PSD analysis on BeiDou and GPS 10 Hz dynamic data for change detection *Adv. Space Res.* **59** 2794–808
Schmid R, Dach R, Collilieux X, Jäggi A, Schmitz M and Dilssner F 2016 Absolute IGS antenna phase center model igs08.atx: status and potential improvements *J. Geod.* **90** 343–64
Schnorr C P and Euchner M 1994 Lattice basis reduction: improved practical algorithms and solving subset sum problems *Math. Program.* **66** 181–99
Schönemann P H 1964 A solution of the orthogonal procrustes problem with applications to orthogonal and oblique rotation *PhD Thesis* University of Illinois
Schönemann P H 1966 A generalized solution of the orthogonal procrustes problem *Psychometrika* **31** 1–10
Seeber G 2003 *Satellite Geodesy* 2nd edn (Berlin: Walter de Gruyter)

Shu Y M, Shi Y, Xu P L, Niu X J and Liu J N 2017 Error analysis of high-rate GNSS precise point positioning for seismic wave measurement *Adv. Space Res.* **59** 2691–713
Shuster M D 1990 Kalman filtering of spacecraft attitude and the QUEST model *J. Astronaut. Sci.* **38** 377–93
Shuster M D and Oh S D 1981 Three-axis attitude determination from vector observations *J. Guid. Control* **4** 70–7
Takeo M 2009 Rotational motions observed during an earthquake swarm in April 1998 offshore Ito, Japan *Bull. Seismol. Soc. Am.* **99** 1457–67
Teunissen P 1995 The least-squares ambiguity decorrelation adjustment: a method for fast GPS integer ambiguity estimation *J. Geod.* **70** 65–82
Teunissen P 2012a The affine constrained GNSS attitude model and its multivariate integer least-squares solution *J. Geod.* **86** 547–63
Teunissen P 2012b A-PPP: array-aided precise point positioning with global navigation satellite systems *IEEE Trans. Signal Process.* **60** 2870–81
Umeyama S 1997 Least squares estimation of transformation parameters between two point patterns *IEEE Trans. Pattern Anal. Mach. Intell.* **13** 376–80
Van Graas F and Braasch M 1991 GPS interferometric attitude and heading determination: initial flight test results *Navigation* **38** 297–316
Waegli A and Skaloud J 2009 Optimization of two GPS/MEMS-IMU integration strategies with application to sports *GPS Solut.* **13** 315–26
Wahba G 1965 A least squares estimate of spacecraft attitude *SIAM Rev.* **7** 409
Wang B, Miao L, Wang S and Shen J 2009 A constrained LAMBDA method for GPS attitude determination *GPS Solut.* **13** 97–107
Xu P L 2001 Random simulation and GPS decorrelation *J. Geod.* **75** 408–23
Xu P L 2006 Voronoi cells, probabilistic bounds and hypothesis testings in mixed integer linear models *IEEE Trans. Inf. Theory* **52** 3122–38
Xu P L 2012 Parallel Cholesky-based reduction for the weighted integer least squares problem *J. Geod.* **86** 35–52
Xu P L 2013 Experimental quality evaluation of lattice basis reduction methods for decorrelating low-dimensional integer least squares problems *EURASIP J. Adv. Signal Process.* **2013** 137
Xu P L 2015 Mixed integer linear models *Handbook of Geomathematics* 2nd edn, ed W Freeden *et al* (Berlin: Springer) pp 2405–51
Xu P L, Shi C and Liu J N 2012 Integer estimation methods for GPS ambiguity resolution: an applications-oriented review and improvement *Surv. Rev.* **44** 59–71
Xu P L, Shi C, Fang R, Liu J N, Niu X J, Zhang Q and Yanagidani T 2013 High-rate precise point positioning (PPP) to measure seismic wave motions: an experimental comparison of GPS PPP with inertial measurement units *J. Geod.* **87** 361–72
Yigit C 2016 Experimental assessment of post-processed kinematic precise point positioning method for structural health monitoring *Geomatics Nat. Hazards Risk* **7** 360–83